Novel monoclonal antibody-based enzyme immunoassay for determining plasma levels of ADAMTS13 activity

Seiji Kato, Masanori Matsumoto, Tomomi Matsuyama, Ayami Isonishi, Hisahide Hiura, and Yoshihiro Fujimura

BACKGROUND: ADAMTS13 specifically cleaves unusually large von Willebrand factor (VWF) multimers, which induce platelet thrombi formation under high shear stress. ADAMTS13 activity is deficient in patients with thrombotic thrombocytopenic purpura (TTP). The determination of plasma levels of ADAMTS13 activity is a prerequisite for a differential diagnosis of thrombotic microangiopathies. Here, a unique and highly sensitive enzyme immunoassay (EIA) of ADAMTS13 activity is described.

STUDY DESIGN AND METHODS: ADAMTS13 hydrolyzes the peptide bond between Y1605 and M1606 of VWF. In this assay, a recombinant fusion protein (GST-VWF73-His) is used as a substrate. A panel of mouse monoclonal antibodies (MoAbs) that specifically recognizes Y1605, which is the C-terminal edge residue of the VWF-A2 domain and is generated by the enzymatic cleavage, has been produced. These antibodies were prepared with a synthetic decapeptide, termed N-10 (1596-DREQAPNLVY-1605), as the immunogen. Twenty-six clones specific to N10 were obtained, and one anti-N10 MoAb was used in this study.

RESULTS: With horseradish peroxidase–conjugated anti-N10 MoAb, a standard enzyme assay was established. This assay was highly sensitive, and the detection limit was 0.5 percent of the normal. Further, an inhibitor of ADAMTS13 was measured to a level of 0.1 Bethesda units per mL. ADAMTS13 activity was measured in 20 patients with Upshaw-Schulman syndrome, a congenital TTP, and 61 acquired TTP patients. The activity measured by this assay and by the classic VWF multimer assay showed high correlation.

CONCLUSION: A convenient and highly sensitive EIA for ADAMTS13 activity has been established. This assay can be introduced for routine laboratory work in transfusion medicine.

Thrombotic thrombocytopenic purpura (TTP) is a life-threatening disorder characterized by Moschcowitz's pentad of thrombocytopenia, microangiopathic hemolytic anemia, fluctuating neurologic signs, renal impairment, and fever.[1] With the exception of the thrombocytopenia, however, recent studies have indicated that clinical features of TTP are highly heterogeneous.[2,3] This observation has become solid after a discovery of von Willebrand factor (VWF)-cleaving protease or ADAMTS13 (a disintegrin-like and metalloproteinase with thrombospondin type 1 motif 13).[4-9] A laboratory diagnosis of TTP is now made upon measurement of plasma ADAMTS13 activity,[10,11] congenitally conferred by mutations in the ADAMTS13 gene in Upshaw-Schulman syndrome (USS)[12] or acquired after the development of neutralizing and/or nonneutralizing autoantibodies.

ADAMTS13 is primarily produced by the stellate cells of liver (Itoh cells) and then thought to be released into circulation via the microsinusoidal system.[13] Under the physiologically high shear stresses of this site, ADAMTS13

ABBREVIATIONS: BU(s) = Bethesda unit(s); GST = glutathione *S*-transferase; His = histidine; TMA(s) = thrombotic microangiopathy(-ies); TTP = thrombotic thrombocytopenic purpura; USS = Upshaw-Schulman syndrome; WB(s) = Western blot(s).

From the Department of Blood Transfusion Medicine, Nara Medical University, Nara; and the Research Institute of Japan Clinical Laboratory, Kyoto, Japan.

Address reprint requests to: Yoshihiro Fujimura, MD, Department of Blood Transfusion Medicine, Nara Medical University, 840 Shijo-cho, Kashihara City, Nara, 634-8522, Japan; e-mail: yfujimur@naramed-u.ac.jp.

This work was supported in part by research grants from the Japanese Ministry of Education, Culture, and Science (to Y.F. and M.M.) and the Ministry of Health and Welfare of Japan for Blood Coagulation Abnormalities H17-02 (to Y.F.).

Received for publication November 18, 2005; revision received January 16, 2006, and accepted January 22, 2006.

doi: 10.1111/j.1537-2995.2006.00914.x

TRANSFUSION 2006;46:1444-1452.

specifically cleaves the Y1605-M1606 bond of the VWF-A2 domain. Deficiency of this enzyme results in the accumulation of unusually large VWF multimers in the circulation that can lead to platelet (PLT) aggregation.[14]

During the past decade, assessment of plasma ADAMTS13 activity was performed by an electrophoretic technique with purified VWF as a substrate. This method required a relatively long reaction time in the presence of protein denaturants, such as 1 to 1.5 mol per L urea or guanidine-HCl.[10,11] More recent studies, however, have used *Escherichia coli*–expressed recombinant VWF-A2 polypeptides, tagged with glutathione *S*-transferase (GST)-histidine (His; GST-VWF73-His) or His-T100 (His-VWF188-T100), as the substrate for ADAMTS13 cleavage in the absence of protein denaturants; these changes have dramatically shortened the reaction time.[15-17] In both the classic and the modern assays, however, the principle for determination of ADAMTS13 activity is based on the quantification of residual undigested substrate. A recently introduced FRETS-VWF73 assay with a fluorogenic substrate,[18] unlike other previously reported assays, directly measures the final product generated by ADAMTS13 cleavage. These assays, however, are not sensitive enough to measure the low levels (approx. 5%) of plasma ADAMTS13 activity. Distinction of these levels is critically important to understand the manifestation of the clinical signs of TTP. In addition, this FRETS-VWF73 assay requires a fluorophotometer, which uncommon in routine diagnostic laboratories.

We have developed a highly sensitive enzyme-linked immunosorbent assay (ELISA) measuring ADAMTS13 activity. First, we prepared specific monoclonal antibodies (MoAbs) directed against the decapeptide of the VWF-A2 domain ending with the C-terminal edge residue Y1605, which is generated by ADAMTS13 cleavage. These MoAbs did not react with intact VWF, but did react with the synthetic decapaptide as well as the monomeric or dimeric N-terminal VWF polypeptide (residues 764-1605). Thus, the peroxidase-labeled MoAb could be used as a detection antibody with recombinant VWF73 (residues 1596-1668 of VWF subunit), tagged with both GST and a His tag (GST-VWF73-His),[15] as the enzyme substrate in this novel ELISA. Because this assay would be completed within 3 hours under the hospital environments, it can be introduced for routine laboratory work in transfusion medicine.

MATERIALS AND METHODS

Assays of ADAMTS13 activity and its inhibitors by VWF multimer analysis

We performed a classic VWF multimer assay to screen plasma samples for ADAMTS13 activity and the presence of inhibitors.[10,12] The detection limit of this method for ADAMTS13 activity was 3 percent of the normal levels. The inhibitor titers are expressed as Bethesda units (BUs),[19] where one inhibitor unit is defined as the amount necessary to reduce ADAMTS13 activity to 50 percent of control levels. A titer of greater than 0.5 BUs per mL was considered to be significant. Before assessing the levels of ADAMTS13 inhibitor, test plasma samples were heat-treated at 56°C for 1 hour to kill endogenous ADAMTS13 activity. After centrifugation, the supernatants were examined by these assays.

Patients and their plasma samples

Patient plasma samples were collected from referring hospitals across Japan, along with the patients' clinical information. Those plasma samples that fulfilled the diagnostic criteria for thrombotic microangiopathies (TMAs)[20] were used in this study. Measurement of plasma ADAMTS13 activities and inhibitor titers by VWF multimer analysis categorized these patients into three groups: 1) less than 3 percent of ADAMTS13 activity without the presence of an inhibitor (congenital TTP or USS), 2) less than 3 percent of ADAMTS13 activity with an inhibitor present (acquired TTP), and 3) moderately decreased (≥3%) or subnormal ADAMTS13 activity with or without its inhibitor (TMA). Patients with the clinical manifestations of constitutive TMA, but with normal ADAMTS13 activity, which might be caused by abnormalities in Factor H or CD46, were excluded from this study.

According to these classifications, 81 patients were examined in this study. Of these, 29 had developed acquired TTP, 32 exhibited TMA with measurable ADAMTS13 activity level, and 20 had USS. ADAMTS13 gene analysis confirmed that all USS patients were either compound heterozygotes or homozygotes for gene abnormalities in this protease. In addition, 33 relatives of these USS patients were identified as the carriers of ADAMTS13 gene mutations.[21-24]

Citrated PLT-poor plasma samples prepared from these subjects were frozen on dry ice, sent to our laboratory, and stored at –80°C until use. Normal citrated plasma samples were obtained from 55 healthy individuals (29 female and 26 male, aged 20-40 years) for use as controls and frozen in aliquots at –80°C. Pooled normal plasma samples from these individuals was used as standard plasma in this study. These studies were conducted with the approval of the ethics committee of Nara Medical University.

Preparation and cleavage of GST-VWF73-His fusion protein

Recombinant GST-VWF73-His fusion protein was expressed in *E. coli* inclusion bodies and purified by the method of Kokame and colleagues.[15] Purified GST-VWF73-His was cleaved with plasma ADAMTS13 by the incubation of 540 ng of substrate with 1 μL of normal plasma in

a total volume of 100 µL of reaction buffer (5 mmol/L Tris-HCl, 10 mmol/L $BaCl_2$, and 1 mmol/L PMSF, pH 5.5) at 37°C for 1 hour. Reactions were terminated by the addition of 1 µL of ethylenediaminetetraacetate (EDTA)-2Na (500 mmol/L).

Production of anti-N10 and N15 murine MoAbs

Two synthetic peptides were designed for use as immunogens in the production of MoAbs, a decapeptide (1596-DREQAPNLVY-1605, termed N10) derived from the VWF-A2 domain and a pentadecapeptide (1596-DREQAPNLVYMVTGN-1610, termed N15). Both peptides were conjugated to keyhole limpet hemocyanin (Asahi Techno Glass Corp., Tokyo, Japan). Four 8-week-old Balb/c mice were immunized subcutaneously with 50 µg of each peptide emulsified in complete Freund's adjuvant (Wako Pure Chemical Industries, Ltd., Osaka, Japan). Three immunizations were performed at 2-week intervals. A final booster was given intraperitoneally at a concentration of 10 µg per 100 µL in saline solution at 2 weeks after the last immunization. Mice splenocytes were fused with myeloma cells (P3U1 cell line) according to the method of Köhler and Milstein.[25] Screening of positive hybridomas was performed by ELISA of culture supernatants in polystyrene microtiter plates coated with the recombinant peptides.

Conjugation of horseradish peroxidase to MoAb

Antibodies were purified from culture supernatants of hybridoma cells with a protein A-Sepharose Fast Flow column (Amersham Bioscience, Corp., Piscataway, NJ). Fractions containing immunoglobulin G (IgG) were pooled and dialyzed against PBS. Purified monoclonal IgG was digested with pepsin; the resulting $F(ab')_2$ fragments were purified by the method of Hamaguchi and associates[26] and conjugated to horseradish peroxidase (HRP).[27]

Western blot analysis

Sodium dodecyl sulfate–polyacrylamide gel electrophoresis (SDS-PAGE) was performed with either a Tris-glycine buffer system[28] or a Tris-tricine buffer system.[29] After electrophoresis, separated proteins were electrophoretically transferred to polyvinylidene fluoride (PVDF) membranes (Bio-Rad, Hercules, CA). After blocking nonspecific binding with 3 percent skim milk, PVDF membranes were incubated with monoclonal IgGs. When indicated, the monoclonal IgGs were labeled with HRP; for unlabeled monoclonal IgGs, bound antibody was detected with peroxidase-labeled anti-mouse IgG. Proteins were visualized by chemiluminescence with Western lightning chemiluminescence reagent (Perkin-Elmer Life Sciences, Inc., Boston, MA) and imaged by X-ray autoradiography (Eastman Kodak, Rochester, NY).

ELISA for ADAMTS13 activity with anti-N10 MoAb

One-hundred microliters of GST-VWF73-His solution (250 ng/mL in PBS with 1 percent BSA) was added to each well of microtiter plates coated with an anti-GST polyclonal antibody (Rockland Immunochemicals, Inc., Gilbertsville, PA) and incubated at 37°C for 1 hour. After three washes with PBS-0.05 percent Tween 20 (PBS/T), 100 µL of each sample, plasma diluted 11-fold in reaction buffer (5 mmol/L acetate buffer and 5 mmol/L $MgCl_2$, pH 5.5) was incubated in the wells at 37°C for 1 hour. After washing the wells three times with PBS/T, 100 µL of HRP-conjugated anti-N10 MoAb (No. 146) was added and incubated at 37°C for 1 hour. Wells were then washed three times with PBS/T. One-hundred microliters of HRP substrate (*o*-phenylendiamine-H_2O_2) was added and incubated for 10 minutes. The reaction was terminated with 100 µL of 1 mol per L H_2SO_4; absorbance was then measured at 492 nm. To generate a reference curve, pooled normal plasma serially diluted in heat-immobilized plasma was assessed. To determine sample activity in plasma, the optical density of the test sample was interpolated against the reference curve. The ADAMTS13 inhibitor titer was measured by the combination of this ELISA with a Bethesda method.

Anti-ADAMTS13 murine MoAb

Two anti-ADAMTS13 murine MoAbs, termed A10 and C7, were produced in our laboratory as previously reported.[13] Of these, A10 completely inhibited plasma ADAMTS13 activity at a final concentration of 50 µg IgG per mL by VWF multimer assay, and the epitope was shown residing on a disintegrin-like domain of ADAMTS13 molecule.[13]

RESULTS

Epitope mapping of anti-N15 and N10 MoAbs

By ELISA-based screening assay, we obtained three MoAb clones specific for peptide N15 and 26 MoAb clones against peptide N10. The reactivity of these MoAbs was also tested by Western blotting (WB) with two GST fusions of VWF, GST-VWF73-His (uncleaved) and GST-VWF10 (cleaved by ADAMTS13; Fig. 1). Clones of anti-N15 MoAbs immunoreacted solely with the intact GST-VWF73-His (35 kDa) and did not react with cleaved GST-VWF10 (30 kDa). In contrast, the clones of anti-N10 MoAbs reacted with the GST-VWF10, but only barely with GST-VWF73-His. We chose two anti-N15 clones (No. 22 and 73) and three anti-N10 clones (No. 116, 146, and 229) for further characterization.

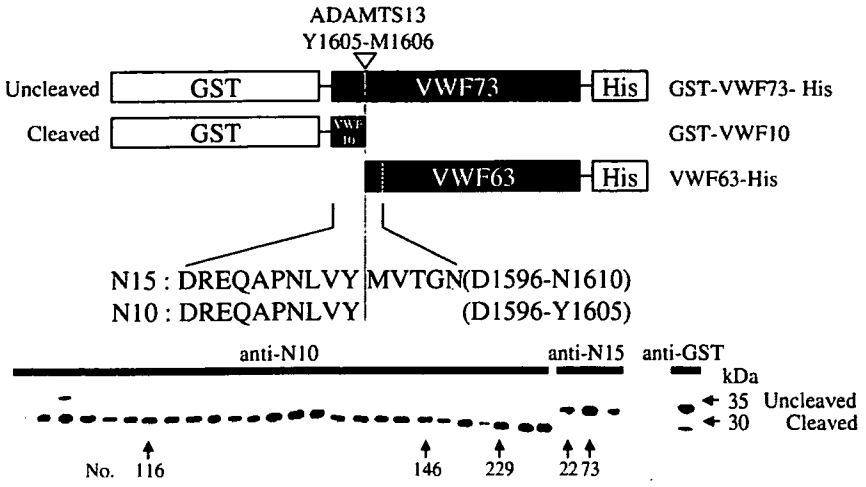

Fig. 1. Production of anti-N10 and anti-N15 murine MoAbs. The schematic structures of the GST-VWF73-His (uncleaved) and GST-VWF10 (cleaved by ADAMTS13) fusions are shown in the top panel. Anti-N10 MoAbs (26 clones), anti-N15 MoAbs (3 clones), and a polyclonal anti-GST antibody serving as a control were used for WB. The anti-N15 clones immunoreacted with the uncleaved GST-VWF73-His band (35 kDa), but not with the cleaved GST-VWF10 (30 kDa). In contrast, the anti-N10 MoAbs reacted with the GST-VWF10, but only minimally with GST-VWF73-His.

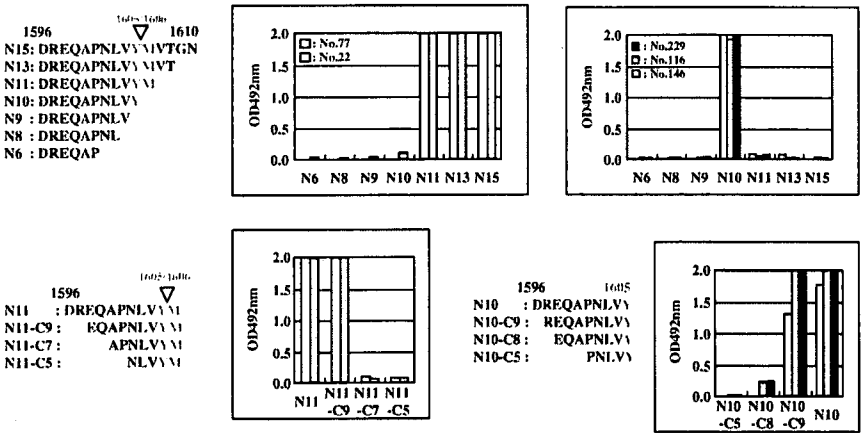

Fig. 2. Epitope mapping of anti-N15 (left) and anti-N10 (right) MoAbs by antigen-immobilized ELISA. For epitope mapping, we tested the immunoreactivities of anti-N15 and anti-N10 MoAbs against a panel of synthetic peptides by ELISA. The immunoreactivities of N15 against the C-terminal truncated peptides are shown in the top panel. The anti-N15 MoAbs reacted with N15 to N11, but lost any interaction upon deletion of M1606. In contrast, the anti-N10 MoAbs specifically reacted with N10 only. In the bottom panel, the reactivity of the anti-N15 and anti-N10 MoAbs with N-terminally deleted N11 and N10 peptides were shown. The anti-N15 MoAbs completely lost their immunoreactivity with the deletion of the four N-terminal residues (D1596 to Q1599) from the N11 peptide. The anti-N10 MoAbs lost their immunoreactivity upon deletion of the two N-terminal residues (D1596 and R1597).

To determine the precise epitopes recognized by these MoAbs, we tested the immunoreactivity of anti-N15 and anti-N10 MoAbs for a panel of synthetic peptides by ELISA (Fig. 2). The two anti-N15 MoAbs shared epitopes within amino acid residues 1596-DREQAPNLVYM-1606 of the VWF-A2 subunit, which required the presence of the two adjacent residues (1605-YM-1606). In contrast, three anti-N10 MoAbs consistently recognized epitopes on the 1597-REQAPNLVY-1605 peptide. For the anti-N10 MoAbs, the presence of Y1605 as the C-terminal residue was an absolute requirement; neither of these MoAbs reacted with the N11 or N9 peptides. Deletion of the two N-terminal residues (D1596 and R1597) from the N10 peptide resulted in an almost complete loss of immunoreactivity with the three anti-N10 MoAb clones. Thus, the epitopes recognized by the anti-N10 MoAbs consistently reside within the 1597-REQAPNLVY-1605 peptide. Hereafter, two MoAbs, one anti-N10 (No. 146) and one anti-N15 (No. 22), were used for further studies.

Immunoreactivity of anti-N15 and anti-N10 MoAbs with VWF fragments generated by ADAMTS13 cleavage

Cleavage of purified VWF by rADAMTS13 generated two major fragments with molecular weights of 340 kDa (C-terminal dimer of VWF subunits of residues 1606-2813) and 280 kDa (N-terminal dimer of VWF subunits of residues 764-1605), analyzed by a SDS-5 percent PAGE under nonreducing conditions. Reducing conditions, however, displayed two distinct bands of 140 kDa (a monomer of VWF residues 764-1605) and 176 kDa (a monomer of VWF residues 1606-2813; Fig. 3). We analyzed these rADAMTS13-cleaved VWF fragments by WB with the anti-N10 and N15 MoAbs.

The anti-N10 MoAb reacted exclusively with the 280-kDa fragment and did not react with the 340-kDa fragment under nonreducing conditions. Under reducing conditions, the anti-N10 MoAb reacted with the 140-kDa fragment, but not with the 176-kDa fragment.

In contrast, the anti-N15 MoAb did not react with VWF either before or after cleavage by rADAMTS13 in either nonreducing or reducing conditions. These results

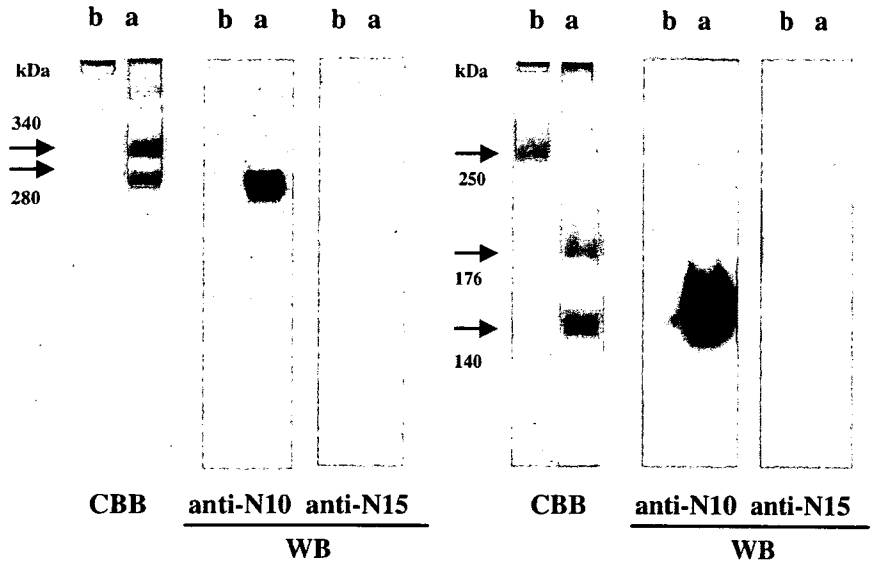

Fig. 3. Immunoreactivity of anti-N10 and anti-N15 MoAbs against VWF fragments generated by ADAMTS13 cleavage. Cleavage of purified VWF by recombinant ADAMTS13 generated two major fragments with molecular weights of 340 kDa (C-terminal dimer of VWF subunit) and 280 kDa (N-terminal dimer of VWF subunit) by a SDS-5 percent PAGE under nonreducing conditions (left). Under reducing conditions (right), two bands corresponding to the N-terminal 140-kDa fragment and the C-terminal 176-kDa fragment could be seen. WB analysis of these VWF fragments before (b) and after (a) cleavage by recombinant ADAMTS13 was performed with the anti-N10 (No. 146) and anti-N15 (No. 22) MoAbs. The anti-N10 MoAb reacted exclusively with the 280-kDa fragment, not the 340-kDa fragment, under nonreducing conditions. Under reducing conditions, the anti-N10 MoAb reacted with the 140-kDa fragment, but not with the 176-kDa fragment or the uncleaved 250-kDa VWF. In contrast, the anti-N15 MoAb did not react with VWF either before or after cleavage by rADAMTS13, under either nonreducing or reducing conditions.

indicate that the epitope recognized by the anti-N15 MoAb on VWF subunit is cryptic before rADAMTS13-mediated cleavage, but no longer exists after cleavage of the 1605-YM-1606 bond. After SDS-1.2 percent agarose gel electrophoresis of normal plasma, WBs with either the anti-N10 or the anti-N15 MoAbs could not detect the VWF multimeric patterns (data not shown).

Establishment of ELISA for ADAMTS13 activity

When ELISA was performed with pooled normal plasma, as described under Materials and Methods, reactivity measured at OD492 nm increased proportionally to the amount of plasma added (Fig. 4A). This additive effect, however, was not seen when with plasma sample derived from patients with USS or acquired TTP. The reactivity of pooled normal plasma was completely blocked by 10 mmol per L EDTA, but was not abolished by the addition of a protease inhibitor cocktail (effective against a broad range of serine proteases, cysteine proteases, aminopeptidases, and acid proteases; Sigma-Aldrich, Inc., St. Louis, MO).

The optimal conditions for this ELISA were determined with pooled normal plasma. We varied the following conditions in the reaction mixture (Fig. 4B): 1) incubation time for enzymatic cleavage, 2) species of divalent metal ions present, 3) NaCl concentration (ionic strength), 4) Mg^{2+} concentration, 5) urea concentration, and 6) pH. The ELISA was most efficient when performed for 1 hour in 5 mmol per L acetate buffer (pH 5.5) containing 5 mmol per L $MgCl_2$ in the absence of urea. A detection limit of 0.5 percent ADAMTS13 activity was estimated by the intersection point of the curve of minus 2.6 standard deviations (SDs) for the standards measured in 10 replications and the zero standards of plus 2.6 SDs (data not shown). To evaluate the precision of this assay, we measured the ADAMTS13 activities present in three different plasma samples in eight replications (within-run assay). The mean ± SD values of three samples were 4.4 ± 0.4, 52.0 ± 2.1, and 103.2 ± 7.4 percent (n = 8). The coefficient of variation values of three samples were 9.7, 3.9, and 7.1 percent (n = 8), respectively (data not shown).

Effect of antibodies in the novel ELISA

Under the optimal conditions determined above, we examined the effect of antibodies against VWF and ADAMTS13 in this novel ELISA (Fig. 5A). Pooled undiluted normal plasma was incubated for 2 hours at 37°C with varying concentrations of each purified IgG; the residual activity of ADAMTS13 in each mixture was then determined. The purified IgG from normal subjects did not exhibit significant inhibition at any concentration tested, but samples from patients with acquired TTP showed a dose-dependent inhibition, completely abrogating ADAMTS13 activity at a final concentration of 500 μg per mL. Anti-ADAMTS13 MoAb A10 (20 μg IgG/mL, final) totally blocked ADAMTS13 activity in this novel ELISA, as shown in the VWF multimer assay. The anti-N15 MoAb displayed total inhibition of plasma ADAMTS13 activity at a concentration of 20 μg per mL. These results indicate that this novel ELISA can specifically recognize the cleavage of the peptide bond between Y1605 and M1606 of the VWF-A2 domain.

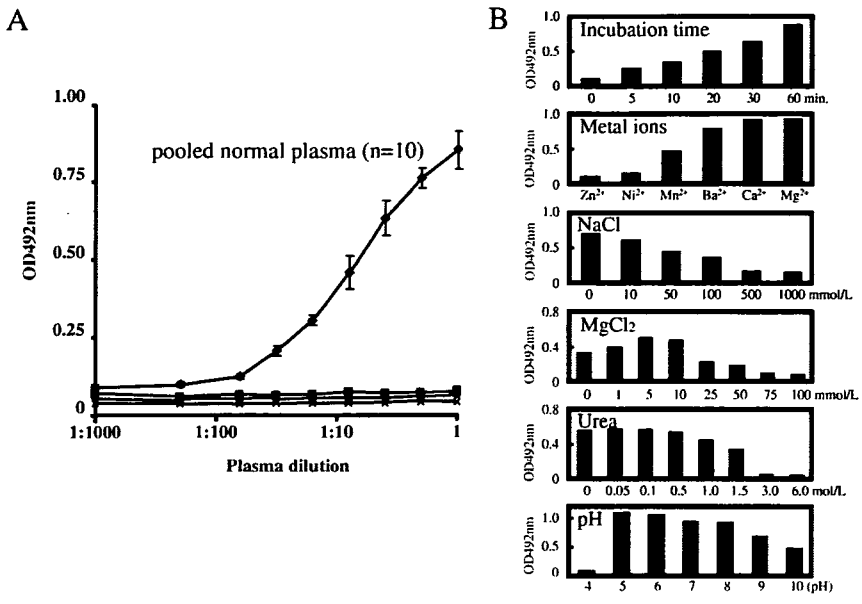

Fig. 4. Establishment of ELISA for ADAMTS13 activity. (A) In this ELISA, intensity at OD492 nm increased in proportion to the normal plasma (◆) concentration. This correlation was not observed for plasma samples from patients with USS (●) or acquired TTP (■) or in the presence of 10 mmol/L EDTA (×). The values for normal plasma shown are the mean and SD (n = 10). (B) Optimal conditions for this ELISA were determined with pooled normal plasma by varying the following conditions: 1) incubation time for enzymatic cleavage, 2) the species of divalent metal ions included (5 mmol/L, final concentration), 3) NaCl concentrations (ionic strength), 4) Mg^{2+} concentrations, 5) urea concentrations, and 6) pH.

Measurement of plasma ADAMTS13 inhibitory activity

We also determined plasma ADAMTS13 inhibitory activity in samples from patients with acquired TTP with this ELISA. We observed a good correlation between the activities of anti-ADAMTS13 inhibitors determined by this ELISA and those given by the VWF multimer assay (Fig. 5B). The detection limit of VWF multimer and ELISA methods were 0.5 and 0.1 BUs per mL, respectively. A significant positive correlation with a coefficient of 0.99 was observed for 38 independent samples.

Levels of plasma ADAMTS13 activity

For 20 patients with USS who consistently exhibited plasma levels of ADAMTS13 activity less than 3 percent of normal levels by a classic VWF multimer assay, the value determined with this novel ELISA was less than 0.5 percent of normal levels in 16 patients. In the remaining 4 patients, the values ranged from 0.6 to 1.3 percent. USS carriers (n = 33) exhibited activities averaging 34.3 ± 12.3 percent (mean ± SD; Fig. 6). We have reported a very rare individual, the father of a patient with USS, who carries two ADAMTS13 gene mutations (R268P/P475S). He consistently exhibited very low levels of plasma ADAMTS13 activity (4.5-7%) by a classic VWF multimer assay.[21] He is now 38 years old, but so far he has no episode of thrombocytopenia or TTP. By our novel ELISA, this individual also showed low plasma ADAMTS13 activity (4.2%).

Of the 61 patients with acquired TTP, 29 patients had less than 3 percent of normal plasma ADAMTS13 activity, while 32 patients exhibited greater than 3 percent by classic VWF multimer assay. In these groups, the levels of plasma ADAMTS13 activity measured by the novel ELISA were 0.7 ± 0.5 and 13.8 ± 10.3 percent, respectively. In normal individuals, plasma level of ADAMTS13 activity measured under these conditions averaged 99.1 ± 21.5 percent (26 male, 97.1 ± 18.1%; 29 female, 100.1 ± 24.4%; Fig. 6).

The ADAMTS13 activities measured by either ELISA or the classic VWF multimer assay were compared for the three groups of USS patients and carriers, patients with acquired TTP, and normal individuals (Fig. 7). The regression line for the three groups were $y = 0.67x + 3.51$, $y = 1.15x + 1.40$, and $y = 0.90x + 10.05$, respectively. The correlation coefficients for the three groups were $r = 0.82$, $r = 0.79$, and $r = 0.85$, respectively.

DISCUSSION

We have developed a convenient and highly sensitive ELISA measuring ADAMTS13 activity. We prepared mouse MoAbs that recognized the C-terminal edge residue Y1605 of the VWF-A2 domain that is exposed by ADAMTS13 cleavage. Two synthetic peptides, N15 and N10, derived from the VWF-A2 domain were prepared and used as immunogens. We have obtained a number of MoAb clones specific for both peptides and used one MoAb from each group for further studies. Anti-N15 MoAb reacted with both the N15 peptide and GST-VWF73-His, but did not react with N10, GST-VWF10, or the 250-kDa VWF subunit, indicating that the epitope includes the 1605-YM-1606 bond within the VWF-A2 domain, which is cryptic in the full-length VWF subunit. In contrast, the anti-N10 MoAb reacted with the N10 peptide, GST-VWF10, the dimer of the N-terminal VWF subunit, and the monomer of the N-terminal 140-kDa band, but did not react with other synthetic peptides, GST-VWF73-His, or the undigested 250-kDa VWF subunit. Studies with a panel of N10-related

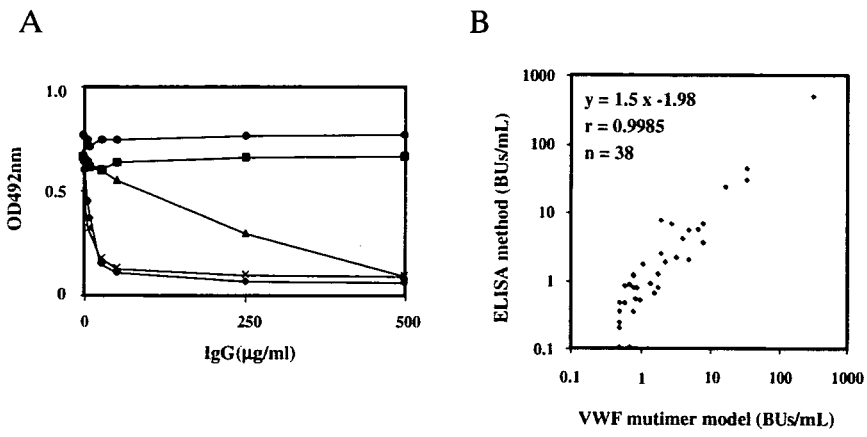

Fig. 5. Effect of antibodies in this ELISA and levels of plasma anti-ADAMTS13 inhibitor. Pooled undiluted normal plasma was incubated for 2 hours at 37°C with varying concentrations of purified IgGs. The residual activity of ADAMTS13 in this mixture was then determined. (A) Purified IgG from normal subjects (■) and normal mouse IgG (●) did not exhibit any significant inhibition at any of the concentrations tested; samples from patients with acquired TTP (▲) demonstrated a dose-dependent inhibition. Of two anti-ADAMTS13 MoAbs generated in this study, both the A10 antibody (×) and the anti-N15 MoAb (No. 73; ◆) completely inhibited ADAMTS13 activity at a concentration of 20 μg/mL. (B) The measurements of anti-ADAMTS13 inhibitor concentration by this ELISA and the VWF multimer assay correlated well. The inhibitor detection limit for the VWF multimer and ELISA methods were 0.5 and 0.1 BUs per mL, respectively. A significant positive correlation with a coefficient of 0.99 was observed for 38 independent samples.

synthetic peptides indicated that the crucial epitope for anti-N10 MoAb requires Y1605 to be the C-terminal residue, but also recognizes a conformation created by the nanopeptide sequence (1597-REQAPNLVY-1605). This recognition pattern allows the use of this MoAb in our novel ELISA, as the C-terminal Y1605 residue is exposed by the cleavage of full-length VWF by ADAMTS13.

When we performed an ELISA with GST-VWF73-His as a substrate and HRP-labeled anti-N10 MoAb as a second antibody, reactivity increased in proportion to the amount of enzyme added. Next we optimized reaction conditions of this ELISA, because ADAMTS13 requires the presence of divalent cations for its activity. In our novel ELISA, Mg^{2+} was most efficient for expressing the proteolytic activity. This result appeared to be slightly different from previous studies, because Ba^{2+} was optimal in the VWF multimer assay with native VWF as substrate,[30] whereas Ca^{2+} was most efficient in FRETS-VWF73 assay. This inconsistency is apparently caused by the difference of substrate species and reaction conditions, including protein denaturants and pH. Thus, we have included 5 mmol per L $MgCl_2$ in the reaction mixture of our assay. We confirmed the specificity of this novel ELISA by inhibition with EDTA and with a variety of well-characterized MoAbs. As a result, this novel ELISA is superior to previously reported assays.

The first advantage of this assay is the increased sensitivity. The lower limit of this assay was determined to be 0.5 percent of the normal control, in contrast to that of conventional assays at 3 to 5 percent. The sensitivity of this assay provided us with new information about USS and acquired TTP. For example, the novel ELISA demonstrated that 16 of 20 USS patients had plasma levels of ADAMTS13 activity below 0.5 percent of the normal control. The remaining 4 patients, however, had the values of 0.6 to 1.3 percent. Interestingly, an asymptomatic carrier with R268P/P475S gene mutations, the father of a USS patient, showed 4.2 percent of the activity by this ELISA. This may indicate that the plasma level of ADAMTS13 activity between 1.3 and 4.2 percent is a range essentially important to regulate the manifestation of clinical signs of TTP, unless other precipitating factors are present. Prophylactic infusions with a small amount of fresh-frozen plasma (approx. 5 mL/kg, every 2-3 weeks) to USS patients, which is effective at preventing the clinical manifestations, may support our speculation. Further, in patients with acquired TTP with less than 3 percent of ADAMTS13 activity by a VWF multimer assay, this ELISA showed that 23 of 29 had ADAMTS13 activity below 0.5 percent, and the remaining six patients had the values of 0.6 to 2.6 percent.

The second advantage of this assay is the sensitivity of measurement for inhibitors of ADAMTS13. The existence of inhibitors of ADAMTS13 is the key to diagnosing acquired TTP. The levels of plasma inhibitors against ADAMTS13 are also an indicator of the efficacy of therapy, typically plasma exchange or corticosteroids, in patients with acquired TTP. It is difficult, however, to determine accurately the low titers of plasma inhibitors of ADAMTS13 with conventional methods. The detection limit for inhibitors in this novel ELISA was calculated at 0.1 BU per mL. Inhibitor levels under 0.5 BU per mL, the lower limit of a VWF multimer assay, were detected in five patients with acquired TTP with this ELISA. Further investigation will be required to identify the significance of low titer inhibitors.

The third advantage of this ELISA is convenience of its performance in hospital environments, because it does not require any special technique or instrument except for standard ELISA equipment routinely used in many laboratories. As a consequence, we have established a convenient and highly sensitive MoAb-based ELISA to measure

ADAMTS13 activity. The values determined by this method correlated well with those determined by classic VWF multimer assay. Because this novel assay utilizes MoAbs, it may be possible to develop a rapid, automated assay to assess ADAMTS13 activity based on this technology.

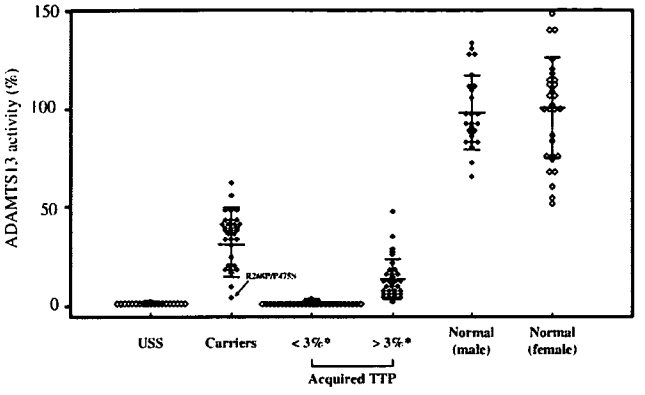

Fig. 6. Plasma levels of ADAMTS13 activity in normal subjects and patients with TTP. Plasma levels of ADAMTS13 activity in 16 patients with USS, determined by the novel ELISA, were less than 0.5 percent of normal levels; in the remaining four patients, activities ranged from 0.6 to 1.3 percent of normal. USS carriers (n = 33) exhibited an average activity of 34.3 ± 12.3 percent (mean ± SD). Of 61 patients with acquired TTP, 29 patients had less than 3 percent and 32 patients displayed greater than 3 percent of normal plasma ADAMTS13 activity by the VWF multimer method. In these two groups, the levels of plasma ADAMTS13 activity by the novel ELISA were 0.7 ± 0.5 and 13.8 ± 10.3 percent, respectively. In normal individuals, our novel ELISA gave a mean plasma ADAMTS13 activity of 99.1 ± 21.5 percent (26 male, 97.9 ± 18.1%; 29 female, 100.1 ± 24.4%).

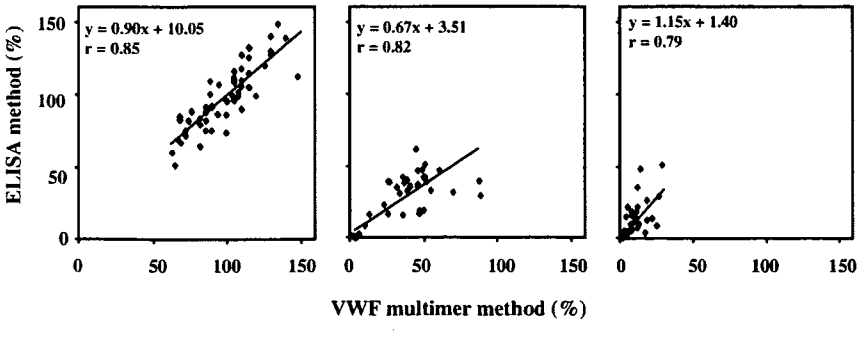

Fig. 7. Correlation of ADAMTS13 activity between ELISA and VWF multimer method. ADAMTS13 activities, measured by ELISA or the VWF multimer method, were compared for samples divided into three groups of patients with USS and carriers (middle, n = 53), patients with acquired TTP (right, n = 61), and normal individuals (left, n = 55). Significant positive correlations were observed in all three groups.

REFERENCES

1. Moschcowitz E. Hyalin thrombosis of the terminal arterioles and capillaries: a hitherto undescribed disease. Proc N Y Pathol Soc 1924;24:21-4.
2. Zheng XL, Kaufman RM, Goodnough LT, Sadler JE. Effect of plasma exchange on plasma ADAMTS13 metalloprotease activity, inhibitor level, and clinical outcome in patients with idiopathic and nonidiopathic thrombotic thrombocytopenic purpura. Blood 2004;103:4043-9.
3. Vesely SK, George JN, Lämmle B, et al. ADAMTS13 activity in thrombotic thrombocytopenic purpura–hemolytic uremic syndrome: relation to presenting features and clinical outcomes in a prospective cohort of 142 patients. Blood 2003;102:60-8.
4. Gerritsen HE, Robles R, Lämmle B, Furlan M. Partial amino acid sequence of purified von Willebrand factor-cleaving protease. Blood 2001;98:1654-61.
5. Fujikawa K, Suzuki H, McMullen B, Chung D. Purification of human von Willebrand factor-cleaving protease and its identification as a new member of the metalloproteinase family. Blood 2001;98:1662-6.
6. Zheng X, Chung D, Takayama TK, et al. Structure of von Willebrand factor cleaving protease (ADAMTS13), a metalloprotease involved in thrombotic thrombocytopenic purpura. J Biol Chem 2001;276:41059-63.
7. Soejima K, Mimura N, Hirashima M, et al. A novel human metalloprotease synthesized in the liver and secreted into the blood: possibly, the von Willebrand factor-cleaving protease? J Biochem 2001;130:475-80.
8. Levy GG, Nichols WC, Lian EC, et al. Mutations in a member of the ADAMTS gene family cause thrombotic thrombocytopenic purpura. Nature 2001;413:488-94.
9. Plaimauer B, Zimmerman K, Volke ID, et al. Cloning expression and characterization of the von Willebrand factor-cleaving protease (ADAMTS13). Blood 2002;100:3626-32.
10. Furlan M, Robles R, Galbusera M, et al. von Willebrand factor-cleaving protease in thrombotic thrombocytopenic purpura and the hemolytic–uremic syndrome. N Engl J Med 1998;339:578-1584.
11. Tsai HM, Lian EC. Antibodies to von Willebrand factor-cleaving protease in acute thrombotic thrombocytopenic purpura. N Engl J Med 1998;339:1585-94.
12. Fujimura Y, Matsumoto M, Yagi H, et al. von Willebrand factor-cleaving protease and Upshaw–Schulman syndrome. In: Progress in Hematology. Int J Hematol 2002;75:25-34.
13. Uemura M, Tatsumi K, Matsumoto M, et al. Localization of ADAMTS13 to the stellate cells of human liver. Blood 2005;106:922-4.

14. Yagi H, Konno M, Kinoshita S, et al. Plasma of patients with Upshaw–Schulman syndrome, a congenital deficiency of von Willebrand factor-cleaving protease activity, enhances the aggregation of normal platelets under high shear stress. Br J Haematol 2001;115:991-7.
15. Kokame K, Matsumoto M, Fujimura Y, Miyata T. VWF73, a region from D1596 to R1668 of von Willebrand factor, provides a minimal substrate for ADAMTS-13. Blood 2004;103:607-12.
16. Zhou W, Tsai HM. An enzyme immunoassay of ADAMTS13 distinguishes patients with thrombotic thrombocytopenic purpura from normal individuals and carriers of ADAMTS13 mutations. Thromb Haemost 2004;91:806-11.
17. Whitelock JL, Nolasco L, Bernardo A, et al. ADAMTS-13 activity in plasma is rapidly measured by a new ELISA method that uses recombinant VWF-A2 domain as substrate. J Thromb Haemost 2004;2:485-91.
18. Kokame K, Nobe Y, Kokubo Y, Okayama A, Miyata T. FRETS-VWF73, a first fluorogenic substrate for ADAMTS13 assay. Br J Haematol 2005;129:93-100.
19. Kasper CK, Aledort LM, Counts RB, et al. A more uniform measurement of factor VIII inhibitors. Thromb Diath Haemorrh 1975;34:869-72.
20. Warkentin TE, Kelton JG. Acquired platelet disorders. In: Bloom AL, Forbes CD, Thomas DP, Tuddenham EG, editors. Hemostasis and thrombosis, Vol. 2. London: Churchill Livingstone; 1994. p. 767-815.
21. Kokame K, Matsumoto M, Soejima K, et al. Mutations and common polymorphisms in ADAMTS13 gene responsible for von Willebrand factor-cleaving protease activity. Proc Natl Acad Sci U S A 2002;99:11902-7.
22. Matsumoto M, Kokame K, Soejima K, et al. Molecular characterization of ADAMTS13 gene mutations in Japanese patients with Upshaw–Schulman syndrome. Blood 2004; 103:1305-10.
23. Uchida T, Wada H, Mizutani M, et al. Identification of novel mutations in ADAMTS13 in an adult patients with congenital thrombotic thrombocytopenic purpura. Blood 2004;104:2081-3.
24. Shibagaki Y, Matsumoto M, Kokame K, et al. Novel compound heterozygote mutations (H234Q/R1206X) of the ADAMTS13 gene in an adult patient with Upshaw–Schulman syndrome showing predominant episodes of repeated acute renal failure. Nephrol Dial Transpl 2006; 21:1289-92.
25. Köhler G, Milstein C. Continuous cultures of fused cells secreting antibody of predefined specificity. Nature 1975;256:495-7.
26. Hamaguchi Y, Yoshitake S, Ishikawa E, Endo Y, Ohtaki S. Improve procedure for the conjugation of rabbit IgG and Fab' antibodies with beta-D-galactosidase from Escherichia coli using N,N'-o-phenylendimaleimidase. J Biochem (Tokyo) 1979;85:1289-300.
27. Yoshitake S, Imagawa M, Ishikawa E, et al. Mild and efficient conjugation of rabbit Fab' and horseradish peroxidase using a maleimide compound and its use for enzyme immunoassay. J Biochem (Tokyo) 1982;92:1413-24.
28. Laemmli UK. Cleavage of structural proteins during the assembly of the head of bacteriophage T4. Nature 1970; 227:680-5.
29. Schägger H, von Jagow G. Tricine-sodium dodesyl sulfate-polyacrylamide gel electrophoresis for the separation of proteins in the range from 1 to 100 kDa. Anal Biochem 1987;166:368-79.
30. Furlan M, Robles R, Lämmle B. Partial purification and characterization of a protease from human plasma cleaving von Willebrand factor to fragments produced by in vivo proteolysis. Blood 1996;87:4223-34.

Journal of Thrombosis and Haemostasis, 4: 1379–1387

ORIGINAL ARTICLE

Critical role of ADP interaction with $P2Y_{12}$ receptor in the maintenance of $\alpha_{IIb}\beta_3$ activation: association with Rap1B activation

T. KAMAE,*[1] M. SHIRAGA,*[1] H. KASHIWAGI,* H. KATO,* S. TADOKORO,* Y. KURATA,† Y. TOMIYAMA* and Y. KANAKURA*

*Department of Hematology and Oncology, Graduate School of Medicine C9, Osaka University; and †Department of Blood Transfusion, Osaka University Hospital, Osaka, Japan

To cite this article: Kamae T, Shiraga M, Kashiwagi H, Kato H, Tadokoro S, Kurata Y, Tomiyama Y, Kanakura Y. Critical role of ADP interaction with $P2Y_{12}$ receptor in the maintenance of $\alpha_{IIb}\beta_3$ activation: association with Rap1B activation. *J Thromb Haemost* 2006; 4: 1379–87

Summary. *Objective:* Platelet integrin $\alpha_{IIb}\beta_3$ plays a crucial role in platelet aggregation, and the affinity of $\alpha_{IIb}\beta_3$ for fibrinogen is dynamically regulated. Employing modified ligand-binding assays, we analyzed the mechanism by which $\alpha_{IIb}\beta_3$ maintains its high-affinity state. *Methods and results:* Washed platelets adjusted to 50×10^3 μL^{-1} were stimulated with 0.2 U mL^{-1} thrombin or 5 μM U46619 under static conditions. After the completion of $\alpha_{IIb}\beta_3$ activation and granule secretion, different kinds of antagonists were added to the activated platelets. The activated $\alpha_{IIb}\beta_3$ was then detected by fluorescein isothiocyanate (FITC)-labeled PAC1. The addition of 1 μM AR-C69931MX (a $P2Y_{12}$ antagonist) or 1 mM A3P5P (a $P2Y_1$ antagonist) disrupted the sustained $\alpha_{IIb}\beta_3$ activation by ~92% and ~38%, respectively, without inhibiting CD62P or CD63 expression. Dilution of the platelet preparation to 500 μL^{-1} also disrupted the sustained $\alpha_{IIb}\beta_3$ activation, and the disruption by such dilution was abrogated by the addition of exogenous adenosine 5′-diphosphate (ADP) in a dose-dependent fashion. The amounts of ADP released from activated platelets determined by high-performance liquid chromatography were compatible with the amounts of exogenous ADP required for the restoration. We next examined the effects of antagonists on protein kinase C (PKC) and Rap1B activation induced by 0.2 U mL^{-1} thrombin. Thrombin induced long-lasting PKC and Rap1B activation. AR-C69931MX markedly inhibited Rap1B activation without inhibiting PKC activation. *Conclusions:* Our data indicate that the continuous interaction between released ADP and $P2Y_{12}$ is critical for the maintenance of $\alpha_{IIb}\beta_3$ activation.

Keywords: $\alpha_{IIb}\beta_3$ activation, adenosine 5′-diphosphate, $P2Y_{12}$, protein kinase C, Rap 1B.

Correspondence: Yoshiaki Tomiyama, Department of Hematology and Oncology, Graduate School of Medicine C9, Osaka University, 2-2 Yamadaoka, Suita Osaka 565-0871, Japan.
Tel.: +81 6 6879 3732; fax: +81 6 6879 3739;
e-mail: yoshi@hp-blood.med.osaka-u.ac.jp

[1]These authors contributed equally to this work.

Received 5 December 2005, accepted 16 February 2006

Introduction

Platelet $\alpha_{IIb}\beta_3$ (GPIIb-IIIa), a non-covalently associated heterodimer, is a prototypic integrin that functions as a physiologic receptor for fibrinogen and von Willebrand factor (VWF). $\alpha_{IIb}\beta_3$ plays a crucial role in platelet aggregation, a key event of hemostatic plug formation and pathologic thrombus formation [1–3]. Inherited abnormalities in the expression or the function of $\alpha_{IIb}\beta_3$ preclude platelet aggregation, resulting in the bleeding disorder Glanzmann thrombasthenia (GT) [4,5]. Conversely, clinical studies have shown the beneficial effects of $\alpha_{IIb}\beta_3$ antagonists in patients undergoing coronary angioplasty or suffering from unstable angina [6,7]. During thrombogenesis, the affinity of $\alpha_{IIb}\beta_3$ for macromolecular ligands is dynamically regulated [1–3]. In resting platelets, $\alpha_{IIb}\beta_3$ is in a low-affinity state and does not bind soluble macromolecular ligands. However, after exposure to the subendothelial matrix, several mediators such as adenosine 5′-diphosphate (ADP) and thromboxane A_2, or shear stress, platelets become activated and activation signals (inside-out signaling) that induce a high-affinity state of $\alpha_{IIb}\beta_3$ for soluble ligands ($\alpha_{IIb}\beta_3$ activation) are generated. So far, much attention has been directed to the nature of inside-out signaling, and major advances have recently been made regarding the structural basis of $\alpha_{IIb}\beta_3$ activation, resulting in the proposal of 'switchblade' and 'deadbolt' models [8,9].

Previous studies revealed that the activation of $\alpha_{IIb}\beta_3$ is a reversible process [10,11]. When platelets are stimulated with weak agonists such as ADP in the absence of fibrinogen, $\alpha_{IIb}\beta_3$ gradually loses its binding capacity. In contrast,

thrombin induces long-lasting $\alpha_{IIb}\beta_3$ activation even in the absence of fibrinogen. Although it has been suggested that the maintenance of $\alpha_{IIb}\beta_3$ activation is mediated by a protein kinase C (PKC)-dependent pathway, the mechanism by which $\alpha_{IIb}\beta_3$ is kept in a high-affinity state still remains elusive [11].

ADP is actively secreted from platelet dense granules upon platelet activation and is passively released from damaged erythrocytes and endothelial cells [12,13]. Platelets possess at least two major G protein-coupled ADP receptors: $P2Y_1$ is a G_q-coupled receptor responsible for mediating platelet shape change and reversible platelet aggregation through intracellular calcium mobilization [14], whereas $P2Y_{12}$ is a G_i-coupled receptor responsible for mediating the inhibition of adenylyl cyclase and sustained platelet aggregation [15,16]. We previously identified a patient with $P2Y_{12}$ deficiency, OSP-1, caused by a point mutation within the translation initiation codon (ATG to AGG) [17]. Based on our findings in the functional analysis of OSP-1 platelets, we thought that $P2Y_{12}$ might play a role in the maintenance of $\alpha_{IIb}\beta_3$ activation.

In this study, employing modified ligand-binding assays we analyzed the mechanism of sustained $\alpha_{IIb}\beta_3$ activation and demonstrated the critical role of the continuous interaction of released ADP with $P2Y_{12}$ receptor in the maintenance of $\alpha_{IIb}\beta_3$ activation.

Materials and methods

Reagents

ADP, protease-activated receptor 1-activating peptide (PAR1 TRAP, SFLLRNPNDKYEPF), PAR 4-activating peptide (PAR4 TRAP, AYPGKF), thrombin, thromboxane A_2 analog U46619 (9, 11-dideoxy-11α, 9α-epoxymethanoprostaglandin $F_{2\alpha}$), apyrase, prostaglandin E_1 (PGE_1), and prostaglandin I_2 (PGI_2) were purchased from Sigma Aldrich (St Louis, MO, USA). Fluorescein isothiocyanate (FITC)-labeled PAC1, a ligand-mimetic $\alpha_{IIb}\beta_3$-specific monoclonal antibody (mAb) that binds specifically to activated $\alpha_{IIb}\beta_3$, was purchased from BD Biosciences (Mountain View, CA, USA) [18]. PE-labeled anti-CD62P (P-selectin), PE-anti-CD63, and PE-IgG were purchased from Beckman Coulter (Fullerton, CA, USA). AR-C69931MX was a generous gift from Astra-Zeneca (Loughborough, UK). Adenosine 3′-phosphate 5′-phosphate (A3P5P) and yohimbine were purchased from Sigma-Aldrich. The specificities and actions of these antagonists have been described [12]. A specific thromboxane A_2 receptor antagonist, SQ-29548, and a PKC inhibitor, Ro31-8220, were purchased from Cayman Chemical (Ann Arbor, MI, USA) and Merck KGaA (Darmstadt, Germany), respectively. MCI-9042, an antagonist for the serotonin ($5\text{-}HT_2$) receptor, was a gift from Mitsubishi Pharma Corporation (Tokyo, Japan) [19]. PT25-2 mAb, which is specific for and activates $\alpha_{IIb}\beta_3$, was a kind gift from Drs Makoto Handa and Yasuo Ikeda (Keio University, Tokyo, Japan) [20]. FK633, an $\alpha_{IIb}\beta_3$-specific antagonist, was kindly provided from Astellas Pharma Inc. (Osaka, Japan) [21].

Platelet preparation

Washed human platelets were prepared as previously described [22]. In brief, fresh whole blood anticoagulated with 0.15 volume of acid–citrate–dextrose solution [National Institute of Health (NIH) formula A] was obtained from healthy volunteers who had not taken any medication for at least 1 week and centrifuged at $250 \times g$ for 10 min to obtain platelet-rich plasma (PRP). After incubation with 20 ng mL^{-1} PGE_1 for 15 min, the PRP was centrifuged at $750 \times g$ for 10 min, washed three times with 0.05 M isotonic citrate buffer containing 20 ng mL^{-1} PGE_1, resuspended in Walsh buffer (137 mM NaCl, 2.7 mM KCl, 1 mM $MgCl_2$, 3.3 mM NaH_2PO_4, 3.8 mM HEPES, 0.1% glucose, 0.1% bovine serum albumin, pH 7.4) without PGE_1, and allowed to rest for 30 min before use.

Flow cytometry

Flow cytometric analysis using monoclonal antibodies (mAbs) was performed as previous described with some modifications [21]. Washed platelets adjusted to 50×10^3 μL^{-1} were stimulated with 0.2 U mL^{-1} thrombin or 5 μM U46619 under static conditions for 15 min. After the stimulation, each of the antagonists or Walsh buffer (for the control) was added to the suspensions for an additional 5 min. The platelet suspensions were then incubated with FITC-PAC1 and PE-anti-CD62P (or PE-anti-CD63) for 30 min and analyzed using a flow cytometer (FACScan; Becton Dickinson, Mountain View, CA, USA).

In another set of experiments, after a 15-min stimulation with thrombin, stimulated platelets were diluted with buffer containing 0.2 U mL^{-1} thrombin or 5 μM U46619 for an additional 5 min. The platelet suspensions were then incubated with FITC-PAC1 for 30 min.

Measurement of released ADP in platelet suspensions by high-performance liquid chromatography (HPLC)

Platelet suspensions (200×10^3 platelets μL^{-1}) were stimulated with thrombin or U46619 for 15 min under static conditions and centrifuged at $1000 \times g$ for 10 min. The supernatant was collected into ultra-free centrifugal filter units (Millipore, Bedford, MA, USA) and centrifuged at $10\,000 \times g$ for 1 min. Then samples were analyzed by HPLC. The chromatographic separation of ADP was performed using the SMART system (Amersham Pharmacia Biotech, Uppsala, Sweden) using an ion-exchange column (mono Q 1.6/5) at room temperature. Aliquots (50 μL) of samples or standard mixtures were injected into the column, and ADP was separated using a gradient in which the concentration of elution buffer B (20 mM Tris–HCl, 1 M NaCl, pH 8.0) was increased from 0% to 50% over a period of 20 min and detected at 254 nm. The

flow rate was 0.1 mL min^{-1} and retention time for ADP was 11.8 min.

Rap 1B activation assay

The detection of activated Rap 1B was performed using a pull-down assay kit according to the manufacturer's instructions (EZ-Detect™ Rap1 Activation Kit; Pierce, Rockford, IL, USA). In brief, platelets that had been prestimulated with 0.2 U mL^{-1} thrombin for 15 min were incubated with 1 μM AR-C69931MX, 1 mM A3P5P, 1 μM PGI_2, or Walsh buffer for 5 min, and then the platelets were lyzed with 0.5% Triton X-100 lysis buffer. The guanosine triphosphate (GTP)-form of Rap 1B was pulled down by incubation with glutathione S-transferase (GST)-RalGDS-Rap 1-binding domain (RBD) and glutathione beads for 1 h at 4 °C. After washing with lysis buffer, proteins were eluted from the precipitates with sodium dodecyl sulfate (SDS)-sample buffer with 2-mercaptoethanol at 100 °C for 5 min, and resolved by electrophoresis on a 12% SDS–polyacrylamide gel electrophoresis. After transfer to polyvinylidene fluoride membranes, Rap 1B was detected with rabbit anti-Rap 1B polyclonal antibody. The total Rap 1B in each lysate was detected in samples assayed in parallel. The optical density of the bands was measured using NIH IMAGE software (Bethesda, MD, USA).

PKC activation assay

PKC activation in thrombin-stimulated platelets was detected by immunoblotting using antiphosphoserine PKC substrate antibody (Cell Signaling Technology, Inc., MA, USA). Conventional PKC isozymes phosphorylate substrates contain serine or threonine, with arginine or lysine at the −3,−2 and +2 positions, and hydrophobic amino acids at position +2. This antibody recognizes conventional PKC substrates only when phosphorylated at the serine residues.

Results

Agonist-induced $\alpha_{IIb}\beta_3$ activation on $P2Y_{12}$-deficient platelets

We previously identified a patient with $P2Y_{12}$-deficiency (OSP-1) as result of a homozygous mutation within the translation initiation codon (ATG to AGG) [17]. We stimulated OSP-1 platelets with different kinds of agonists in the presence of FITC-PAC1 for 30 min and then analyzed PAC1 binding using flow cytometry. As shown in Fig. 1, the amount of PAC1 binding to OSP-1 platelets stimulated with 100 μM PAR1-TRAP, 200 μM PAR4-TRAP or 5 μM U46619 was only 12.5% ± 1.1%, 4.6% ± 0.1% and 4.3% ± 2.3% of the control value (mean ± SD, $n = 4$), respectively. In contrast, phorbol 12-myristate 13-acetate (PMA)-induced PAC1 binding was only slightly impaired (92.9% ± 1.9% of control, mean ± SD, $n = 4$). PAR1-TRAP and U46619 are able to induce transient aggregation of OSP-1 platelets, indicating that $\alpha_{IIb}\beta_3$ could be transiently activated with these agonists [17].

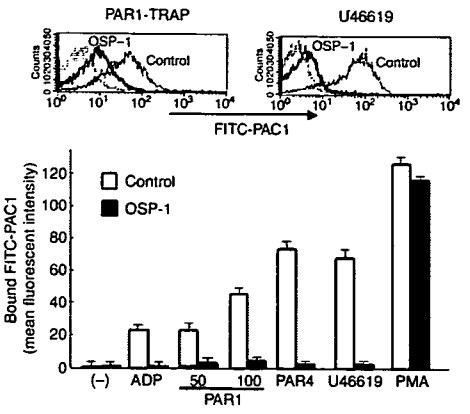

Fig. 1. Agonist-induced $\alpha_{IIb}\beta_3$ activation on platelets from a $P2Y_{12}$-deficient patient, OSP-1. Washed platelets obtained from a patient with $P2Y_{12}$-deficiency (OSP-1) or control subjects (control) were stimulated with 20 μM adenosine 5′-diphosphate (ADP), 50 or 100 μM PAR1-TRAP, 200 μM PAR4-TRAP, 5 μM U46619, or 0.2 μM phorbol 12-myristate 13-acetate (PMA) in the presence of fluorescein isothiocyanate (FITC)-labeled PAC1, and bound PAC1 was analyzed using flow cytometry after 30 min of incubation. (upper panel) Representative histograms of PAC1 binding with 100 μM PAR1-TRAP or 5 μM U46619 stimulation. PAC1 binding to control platelets in the presence of an $\alpha_{IIb}\beta_3$ antagonist (FK633) is shown by a dotted line. (lower panel) Specific PAC1 binding to OSP-1 (closed columns) or control (open columns) platelets calculated using the following formula is shown ($n = 4$): (MFI in the absence of FK633) − (MFI in the presence of FK633).

These findings suggest that the $\alpha_{IIb}\beta_3$ activation may be too short and unstable to be detected by the PAC1-binding assay. From these findings, we assume that released ADP and $P2Y_{12}$-mediated signaling may play a critical role in the maintenance of $\alpha_{IIb}\beta_3$ activation.

Effects of antagonists on the sustained $\alpha_{IIb}\beta_3$ activation induced by thrombin

First, we examined PAC-1 binding at different time points between thrombin stimulation and FITC-PAC1 addition and confirmed that there was no difference in PAC1 binding between time 0 min (thrombin and PAC1 were added at the same time) and time 15 min (PAC1 was added 15 min after thrombin stimulation) (data not shown) [11]. To determine the role of $P2Y_{12}$-mediated signals in the maintenance of $\alpha_{IIb}\beta_3$ activation, an experimental protocol using platelets preactivated with thrombin was then employed (Fig. 2A). After the completion of $\alpha_{IIb}\beta_3$ activation and the induction of α-granules and lysosome secretion by thrombin, each of antagonists was added to the activated platelets. Under these conditions, the stimulated platelets showed long-lasting $\alpha_{IIb}\beta_3$ activation even in the absence of ligand binding. However, the addition of 1 U mL^{-1} apyrase, 1 μM AR-C69931MX (a $P2Y_{12}$ antagonist) or 1 mM A3P5P (a $P2Y_1$ antagonist) disrupted the sustained $\alpha_{IIb}\beta_3$ activation by 87.1% ± 1.4% (mean ± SD, $n = 3$), 91.7% ± 5.3% (mean ± SD, $n = 6$) and 38.2% ± 10.5% (mean ± SD, $n = 4$), respectively, without inhibiting CD62P or CD63 expression (Fig. 2B,C). In

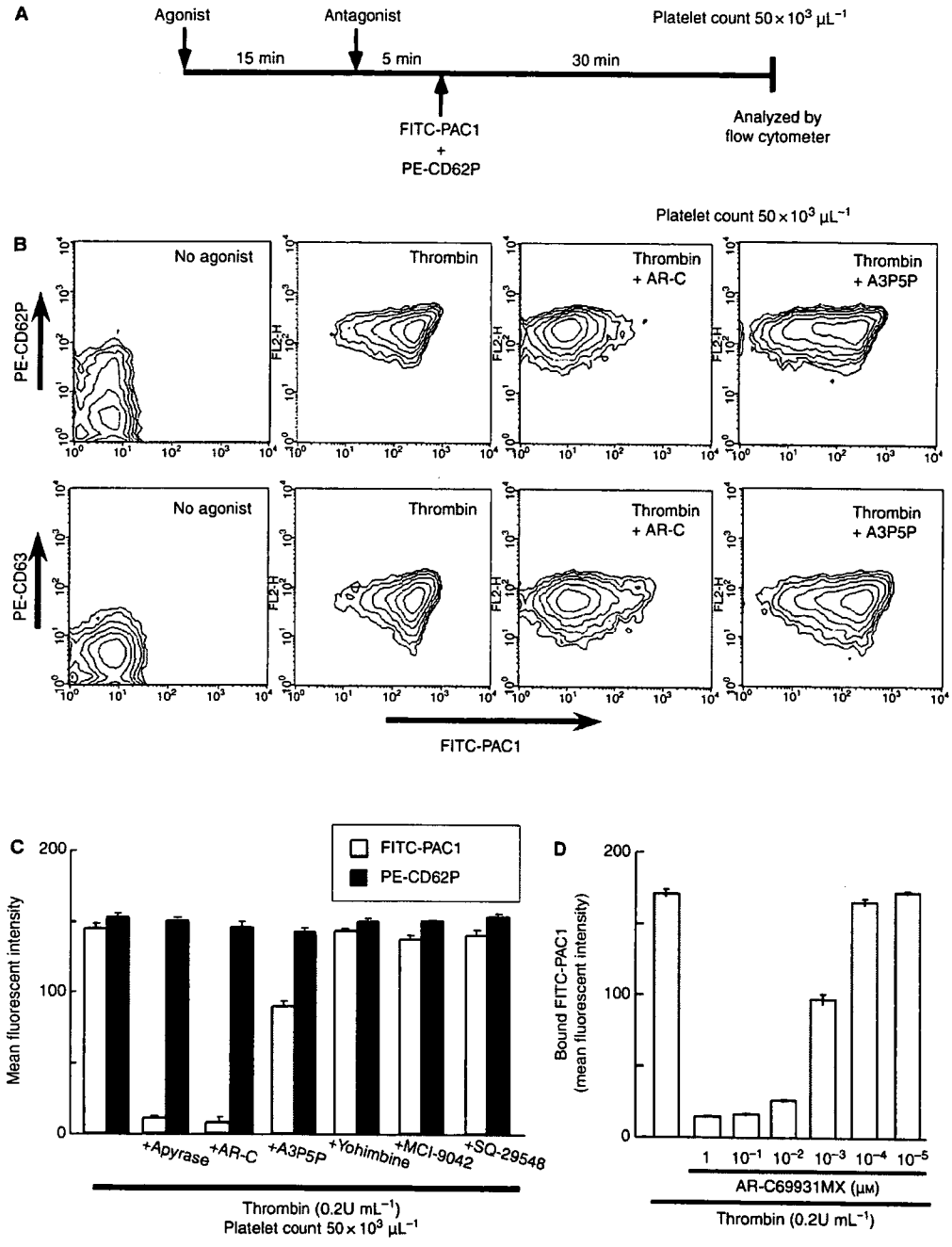

Fig. 2. Effects of receptor antagonists on the sustained $\alpha_{IIb}\beta_3$ activation induced by thrombin. (A) Scheme of the experimental procedure to analyze the effects of antagonists on the sustained $\alpha_{IIb}\beta_3$ activation. (B) One micromolar AR-C69931MX (AR-C) or 1 mM A3P5P was added to thrombin (0.2 U mL^{-1})-stimulated platelets. Representative results obtained using flow cytometry for PAC1 binding and CD62P or CD63 expression are shown. (C) Representative results for specific PAC1 binding in the absence or presence of 1 U mL^{-1} apyrase, 1 mM AR-C, 1 μM A3P5P, 10 μM yohimbine, 1 μM MCI-9042, or 100 nM SQ-29548 (mean ± SD of triplicates) are shown. Similar results were obtained in at least three independent experiments. (D) Dose-dependent inhibition of AR-C on the sustained $\alpha_{IIb}\beta_3$ activation is shown.

addition, AR-C69931MX dose-dependently inhibited the sustained $\alpha_{IIb}\beta_3$ activation with IC_{50} of approximately 1.6 nM (Fig. 2D). This value is very similar to IC_{50} (3.5 nM) for the inhibition of ADP-induced $\alpha_{IIb}\beta_3$ activation [23]. We also examined the effect of 10 μM yohimbine (an adrenergic receptor antagonist), 1 μM MIC-9042 (a 5-HT_2 receptor antagonist) or 100 nM SQ-29548 (a thromboxane A_2 receptor antagonist) on the maintenance of $\alpha_{IIb}\beta_3$ activation. Each of these antagonists showed only negligible effects on PAC1 binding (Fig. 2C).

These results suggest that released endogenous ADP and P2Y$_{12}$ may be required for the maintenance of $\alpha_{IIb}\beta_3$ activation induced by thrombin.

Effects of reduction of the platelet concentration on the sustained $\alpha_{IIb}\beta_3$ activation

Next, we examined if reduction of the released ADP concentration might disrupt the sustained $\alpha_{IIb}\beta_3$ activation. As shown in Fig. 3A, after stimulation with 0.2 U mL^{-1} thrombin for 15 min, platelets (50×10^3 μL^{-1}) were then diluted in Walsh buffer containing 0.2 U mL^{-1} thrombin to produce different platelet concentrations. The reduction of the platelet concentration after thrombin stimulation attenuated PAC1 binding to activated platelets, and PAC1 binding was only 16.9% ± 7.8% of the control value at a concentration of 500 platelets μL^{-1} (83.1% ± 7.8% reduction, mean ± SD, $n = 9$). On the other hand, the addition of PT25-2 mAb to thrombin-activated platelets markedly increased PAC1 binding even at 500 platelets μL^{-1}, indicating that the attenuation of PAC-1 binding is not because of an artifact of the dilution.

Taken together with the data shown in Fig. 2, these results suggest that released component(s), probably ADP, from thrombin-stimulated platelets are critical for the maintenance of $\alpha_{IIb}\beta_3$ activation.

Effects of exogenously added ADP on the sustained $\alpha_{IIb}\beta_3$ activation, and measurement of released ADP by HPLC

To further investigate the role of ADP in the maintenance of $\alpha_{IIb}\beta_3$ activation, we examined the effect of exogenously added ADP on PAC1 binding to platelets at a concentration of 500 platelets μL^{-1}. A series of concentrations of ADP was added to the dilution buffer containing 0.2 U mL^{-1} thrombin. As shown in Fig. 4, the amount of PAC1 binding to platelets was positively correlated with the exogenously added ADP concentration. Even 0.125 μM ADP significantly increased the PAC1 binding, and only approximately 1 μM ADP was sufficient to restore PAC1 binding at 500 platelets μL^{-1} to the levels obtained at 50×10^3 platelets μL^{-1}. The restoration of PAC1 binding by exogenous ADP was almost completely blocked by AR-C69931MX and was partially blocked by A3P5P.

Employing HPLC, we next measured the actual amounts of ADP released from thrombin-stimulated platelets. As shown in Fig. 5, the released ADP concentration was approximately

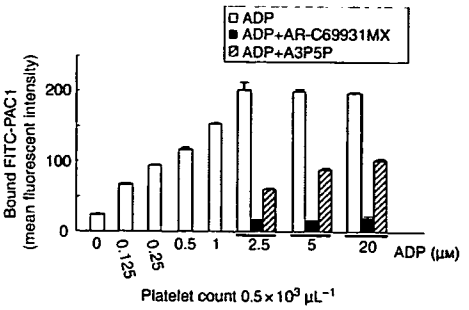

Fig. 4. Effects of exogenously added adenosine 5′-diphosphate (ADP) on the induction of the sustained $\alpha_{IIb}\beta_3$ activation at a platelet concentration of 500 platelets μL^{-1}. After dilution of thrombin (0.2 U mL^{-1})-stimulated platelets to 500 platelets μL^{-1}, the indicated doses of ADP in the absence (open columns) or presence of either 1 μM AR-C69931MX (AR-C, closed columns) or 1 mM A3P5P (shaded columns) were added to the platelet suspension. Representative results for specific PAC1 binding (mean ± SD of triplicates) are shown. Similar results were obtained in three independent experiments.

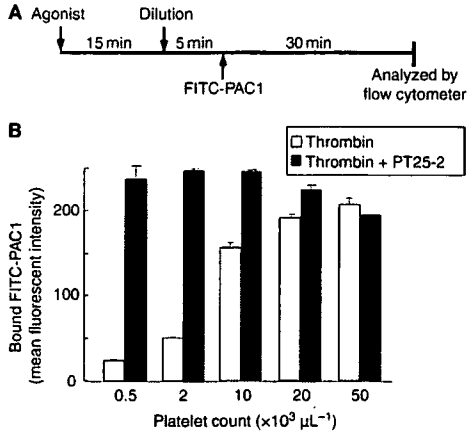

Fig. 3. Effects of platelet dilution on the sustained $\alpha_{IIb}\beta_3$ activation induced by thrombin. (A) Scheme of the experimental procedure to analyze the effects of platelet dilution on the sustained $\alpha_{IIb}\beta_3$ activation. (B) Representative results for specific PAC1 binding to thrombin (0.2 U mL^{-1})-stimulated (open columns) or [thrombin + PT25-2 monoclonal antibody (mAb)]-stimulated platelets (closed columns) at the indicated platelet concentrations (mean ± SD of triplicates) are shown. Similar results were obtained in at least three independent experiments.

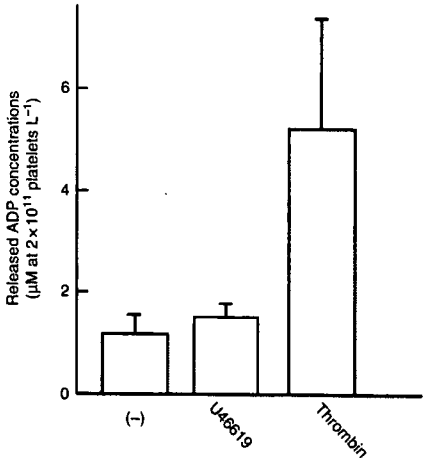

Fig. 5. Measurement of secreted adenosine 5′-diphosphate (ADP) using high-performance liquid chromatography (HPLC). Washed platelets (200×10^3 μL^{-1}) were stimulated with either 5 μM U46619 or 0.2 U mL^{-1} thrombin. After 15 min, platelets were centrifuged at $1000 \times g$ for 10 min, and the concentration of ADP in each supernatant was measured using HPLC as described in Materials and methods ($n = 11$).

5.21 ± 2.17 μM (mean ± SD, $n = 11$) when platelets were stimulated with 0.2 U mL^{-1} thrombin at 2×10^{11} platelets per liter ($=200 \times 10^3$ μL^{-1}). Extrapolation of the data shown in Fig. 5 indicates that an ADP concentration at 50×10^3 μL^{-1} would be approximately 1.30 μM. These values are compatible with the doses of exogenous ADP that restored the PAC1 binding.

Role of $P2Y_{12}$ in sustained $\alpha_{IIb}\beta_3$ activation induced by U46619

We also examined the effect of the released ADP on the sustained $\alpha_{IIb}\beta_3$ activation induced by U46619. The expression levels of CD62P and CD63 as well as the levels of $\alpha_{IIb}\beta_3$ activation on U46619-stimulated platelets were much lower than those on thrombin-stimulated platelets, and not all the platelets expressed CD62P or activated $\alpha_{IIb}\beta_3$. The amount of PAC1 binding was correlated with the CD62P and CD63 expression levels on U46619-stimulated platelets. Again, AR-C69931MX and A3P5P disrupted the U46619-induced sustained $\alpha_{IIb}\beta_3$ activation by 98.7% ± 1.7% and 48.6% ± 10.2%, respectively (mean ± SD, $n = 3$) (Fig. 6). The disruption of PAC1 binding was also induced by reduction of the platelet concentration, and supplementation with approximately 0.25 μM ADP was sufficient to restore PAC1 binding at 500 platelets μL^{-1} to the levels obtained at 50×10^3 platelets μL^{-1} (Fig. 6). The released ADP concentration induced by U46619 stimulation was only 1.51 ± 0.06 μM at 2×10^{11} platelets per liter (mean ± SD, $n = 11$, approximately 0.38 μM at 50×10^3 platelets μL^{-1}) (Fig. 5). These values are also comparable to the doses of exogenous ADP that restored the PAC1 binding level to that induced by U46619. Moreover, higher levels of exogenous ADP further increased the amount of PAC1 binding. These results demonstrate the critical role of released ADP in the sustained $\alpha_{IIb}\beta_3$ activation on U46619-stimulated as well as thrombin-stimulated platelets.

Role of $P2Y_{12}$ in the increase of PKC and Rap1B activities in thrombin-stimulated platelets

In order to further clarify the mechanism by which thrombin induces sustained $\alpha_{IIb}\beta_3$ activation, we examined the effects of AR-C69931MX and A3P5P on the PKC activation induced by thrombin. PKC activation was detected by immunoblot analysis using the antibody specific for phosphorylated serine residues in PKC substrates. As in the experiment shown in Fig. 2A, platelets were stimulated with 0.2 U mL^{-1} thrombin for 15 min, different kinds of antagonists were added for an additional 5 min, and then PKC activation was examined. The phosphorylation of a 47-kDa protein (pleckstrin) was long-lasting, and the addition of AR-C69931MX or A3P5P did not inhibit the phosphorylation of pleckstrin. In contrast, Ro31-8220 markedly inhibited the phosphorylation of pleckstrin (Fig. 7A).

We next examined the activation of Rap1B (GTP-Rap1B) induced by thrombin. Thrombin induced Rap1B activation at 1 min after thrombin stimulation, and the activation was long lasting, even being observed at 30 min (Fig. 7B). In contrast to the PKC activation, AR-C69931MX as well as PGI_2 markedly inhibited the Rap1B activation. However, even in the presence of AR-C69931MX, the addition of epinephrine restored Rap1B activation (Fig. 7C) as well as $\alpha_{IIb}\beta_3$ activation (data not shown).

Discussion

In the present study, we examined the mechanism by which the high-affinity state of $\alpha_{IIb}\beta_3$ is maintained on platelets stimulated with thrombin or U46619 even in the absence of ligand binding. The long-lasting activation of $\alpha_{IIb}\beta_3$ induced by thrombin or U46619 was inhibited by 1 μM AR-C69931MX by 92% and 99%, and by 1 mM A3P5P by 38% and 49%, respectively. Only negligible inhibitory effects were observed with the tested antagonists for adrenergic receptor, 5-HT receptor or thromboxane A_2 receptor. The $\alpha_{IIb}\beta_3$ activation was also inhibited by the dilution of the platelet preparation. The disruption of $\alpha_{IIb}\beta_3$ activation by the dilution was abrogated by the addition of small amounts of exogenous ADP. The concentrations of ADP required for the restoration of $\alpha_{IIb}\beta_3$ activation at 500 platelets μL^{-1} were similar to those of endogenous ADP released from activated platelets [24]. These findings demonstrate that G_q- and $G_{12/13}$-mediated signaling pathways are not sufficient for the sustained $\alpha_{IIb}\beta_3$ activation, and the interaction of secreted ADP with its receptors, especially $P2Y_{12}$, is necessary for the sustained $\alpha_{IIb}\beta_3$ activation induced by thrombin or U46619.

van Willigen and Akkerman have suggested that the sustained $\alpha_{IIb}\beta_3$ activation is tightly controlled by PKC and a cyclic AMP-sensitive process [11]. However, AR-C69931MX disrupted the $\alpha_{IIb}\beta_3$ activation without inhibiting PKC activation when it was added 15 min after stimulation. Thus, $P2Y_{12}$-mediated signaling seems to be a downstream event from PKC activation. PKC activation induces ADP release from dense granules, and then the released ADP additionally induces $P2Y_{12}$-mediated signaling which is essential for the sustained $\alpha_{IIb}\beta_3$ activation. $\alpha_{IIb}\beta_3$ activation was not disturbed by inhibiting thrombin by treatment with hirudin, suggesting that a transient interaction between thrombin and thrombin receptors (PAR-1 and PAR-4) is sufficient for the sustained activation. In sharp contrast, the sustained $\alpha_{IIb}\beta_3$ activation could be disrupted by inhibiting $P2Y_{12}$-mediated signaling even in the presence of thrombin. Desensitization of $P2Y_{12}$ has recently been demonstrated [25]. However, it is likely that the degree of desensitization is not enough to reduce $\alpha_{IIb}\beta_3$ activation under our experimental conditions, as the amounts of activated $\alpha_{IIb}\beta_3$ did not alter even after 15 min of thrombin stimulation. Recently, unique regulation and relocalization of $P2Y_{12}$ after activation have been demonstrated. Although a substantial amount of $P2Y_{12}$ was rapidly and transiently internalized, most of the $P2Y_{12}$ receptors remained at the plasma membrane even after ADP stimulation [26]. Taken together, these findings indicate that the $P2Y_{12}$ remains

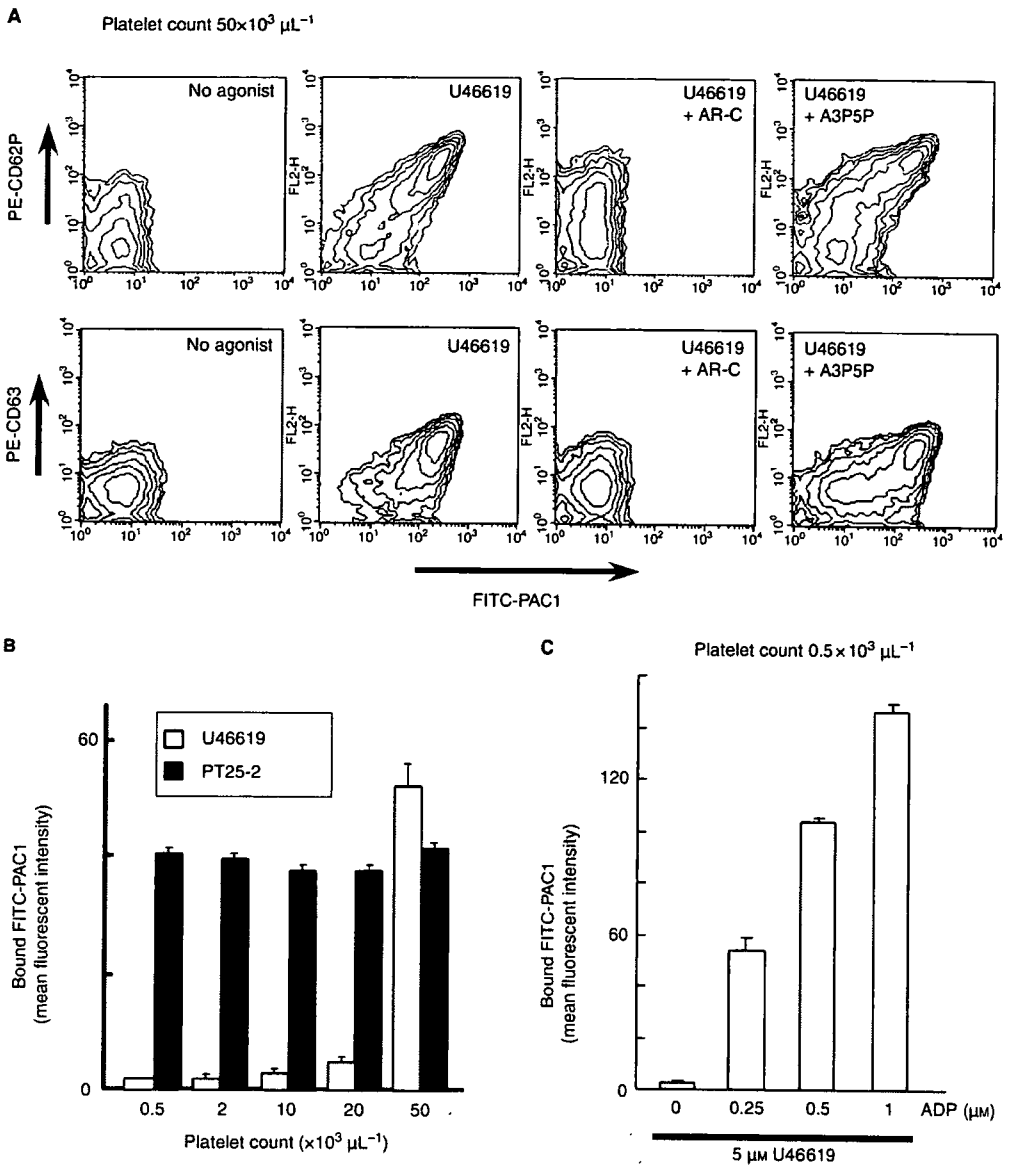

Fig. 6. Sustained $\alpha_{IIb}\beta_3$ activation on platelets stimulated with U46619. (A) Experiments were performed as in Fig. 2 using 5 μM U46619 instead of thrombin. One micromolar AR-C69931MX (AR-C) or 1 mM A3P5P was added to U46619 (5 μM)-stimulated platelets. Representative results obtained using flow cytometry for PAC1 binding and CD62P or CD63 expression are shown. (B) Effects of platelet dilution on the sustained $\alpha_{IIb}\beta_3$ activation induced by U46619. Representative results for specific PAC1 binding to U46619 (5 μM)-stimulated (open columns) or PT25-2-treated platelets (closed columns) at the indicated platelet concentrations (mean ± SD of triplicates) are shown. Similar results were obtained in three independent experiments. (C) Effects of exogenously added ADP on the induction of the sustained $\alpha_{IIb}\beta_3$ activation on U46619-stimulated platelets at a concentration of 500 platelets μL^{-1}. The indicated doses of ADP were added to the U46619-stimulated platelet suspension.

functional after thrombin stimulation and continuous interaction between P2Y$_{12}$ and the released ADP is critical for the sustained $\alpha_{IIb}\beta_3$ activation.

To further clarify the mechanism of the sustained $\alpha_{IIb}\beta_3$ activation by thrombin, we examined the activation of small GTPase Rap 1B during the sustained $\alpha_{IIb}\beta_3$ activation, as Rap 1B has recently been demonstrated to be a regulator of $\alpha_{IIb}\beta_3$ activation in platelets [27]. In response to calcium and DAG, CalDAG-GEFI activates Rap 1B by promoting the release of GDP and the loading of GTP. Both Rap 1B-null mice and CalDAG-GEFI-null mice show impaired $\alpha_{IIb}\beta_3$ activation in response to different kinds of agonists [28,29]. Thrombin induced sustained Rap 1B activation under our experimental conditions. However, the addition of AR-C69931MX as well as PGI$_2$ after a 15-min stimulation disrupted the sustained Rap 1B activation and $\alpha_{IIb}\beta_3$ activation. Because G_z-mediated signaling induced by epinephrine could activate $\alpha_{IIb}\beta_3$ in P2Y$_{12}$-deficient mice [30], we examined the effect of

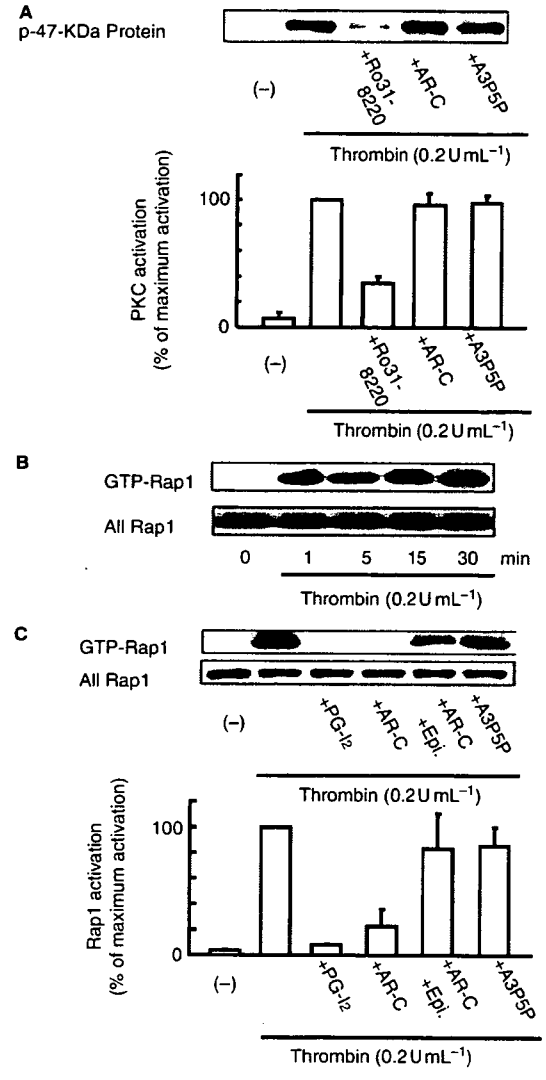

Fig. 7. Effects of $P2Y_{12}$ antagonist on protein kinase C (PKC) and Rap1B activation. (A) (upper panel) Washed platelets (200×10^3 μL^{-1}) were stimulated with 0.2 U mL^{-1} thrombin, and 15 min later 5 μM Ro31-8220, 1 μM AR-C69931MX (AR-C), or 1 mM A3P5P was added to the activated platelets. After 5 min, the platelets were lyzed, and PKC activation was detected by immunoblotting using antiphosphoserine PKC substrate antibody. The phosphorylation of a 47-kDa protein (pleckstrin) is shown. (lower panel) Optical density of the 47-kDa band was measured using NIH IMAGE software, and relative % compared with PKC activation without antagonist (maximum activation) is shown (mean ± SD, $n = 3$). (B) Washed platelets (200×10^3 μL^{-1}) were stimulated with 0.2 U mL^{-1} thrombin, and Rap 1B activation was detected by the pull-down assay using GST-RalGDS-RBD followed by incubation with rabbit anti-Rap 1B polyclonal antibody at indicated time points. Total Rap 1B in each lysate was detected in parallel. (C) (upper panel) Washed platelets (200×10^3 μL^{-1}) were stimulated with 0.2 U mL^{-1} thrombin, and 15 min later 1 μM PGI_2, 1 μM AR-C69931MX (AR-C), 1 μM AR-C + 10 μM epinephrine, or 1 mM A3P5P was added to the activated platelets. After 5 min, the platelets were lyzed, and then Rap 1B activation was examined. (lower panel) Optical density of activated Rap 1B was measured using NIH IMAGE software, and relative % compared with Rap 1B activation without antagonist (maximum activation) is shown (mean ± SD, $n = 3$).

epinephrine under our experimental conditions. Interestingly, the addition of epinephrine induced Rap 1B activation even in the presence of AR-C69931MX. Thus, our data demonstrate that there is a close relationship between the sustained $\alpha_{IIb}\beta_3$ activation and Rap 1B activation. Our data are consistent with previous reports that G_i-mediated signaling is necessary for Rap 1B activation [31,32] and also demonstrate for the first time that the continuous stimulation of G_i-mediated signaling is needed for the sustained Rap 1B activation. The patient with $P2Y_{12}$ deficiency (OSP-1) showed the markedly impaired PAC-1 binding in response to different kinds of agonists except for PMA, which is similar to CalDAG-GEFI-null mice [28]. It is possible that PMA may induce CalDAG-GEFI (and Rap1B)-independent signaling pathways to induce and sustain $\alpha_{IIb}\beta_3$ activation [28].

Our present findings also indicate important cautions regarding $\alpha_{IIb}\beta_3$ ligand binding assays. Platelet concentrations and the timing of ligand incubation could influence the ligand-binding capacity of $\alpha_{IIb}\beta_3$. This is especially true of U46619 stimulation, because the amount of ADP released from U46619-stimulated platelets was much lower than that released from thrombin-stimulated platelets. Indeed, the ligand-binding capacity of U46619-stimulated platelets was dramatically influenced by the platelet concentration. In addition, the presence of leukocytes in PRP or whole blood may also modify the results, as leukocyte ecto-nucleotidase (CD39) influences the metabolism of released ADP [33]. Thus, several factors influencing the concentration of released ADP should be taken into account during $\alpha_{IIb}\beta_3$ ligand-binding assays.

A number of studies, including ours, have demonstrated the important role of $P2Y_{12}$ in thrombus stability [17,30,34]. Moreover, recent *in vivo* observations demonstrated that during platelet thrombus formation, circulating platelets were tethered to the luminal surface of growing thrombi by VWF–GPIb interaction. However, more than 95% of tethered platelets were subsequently translocated and/or detached [35,36]. In this study, we obtained the novel finding that the $\alpha_{IIb}\beta_3$ activation could not be sustained at a low concentration of platelets (500 platelets μL^{-1}) without exogenous ADP. Activated $\alpha_{IIb}\beta_3$ on the detached platelets should become inactivated, because the released ADP is immediately diluted by the blood flow. At the luminal surface, activated $\alpha_{IIb}\beta_3$ on the tethered platelets would be maintained only when the platelets are continuously exposed to ADP released from adjacent activated platelets. At the inside of growing thrombi, it appears that platelets are constantly exposed to such high concentrations of released ADP that $\alpha_{IIb}\beta_3$ can be maintained in its high-affinity state in concert with the effects of thrombin and TXA_2. It is possible that ADP concentrations surrounding platelets may largely influence on determining whether platelets participate in thrombus formation or not. Thus, $P2Y_{12}$ may serve as a sensor for thrombogenic status surrounding individual platelets.

In summary, our data demonstrate that the continuous interaction between released ADP and $P2Y_{12}$ is critical for

sustained $\alpha_{IIb}\beta_3$ activation in platelets activated via G_q and $G_{12/13}$-coupled receptors.

Acknowledgements

This study was supported in part by a Grant-in-Aid for Scientific Research from the Ministry of Education, Culture, Sports, Science and Technology in Japan, from the Ministry of Health, Labor and Welfare in Japan; and by a grant from Mitsubishi Pharma Research Foundation, Osaka, Japan.

References

1 Phillips DR, Charo IF, Scarborough RM. GPIIb-IIIa: the responsive integrin. *Cell* 1991; **65**: 359–62.
2 Hynes RO. Integrins: bidirectional, allosteric signaling machines. *Cell* 2002; **110**: 673–87.
3 Shattil SJ, Newman PJ. Integrins: dynamic scaffolds for adhesion and signaling in platelets. *Blood* 2004; **104**: 1606–15.
4 George JN, Caen JP, Nurden AT. Glanzmann's thrombasthenia: the spectrum of clinical disease. *Blood* 1990; **75**: 1383–95.
5 Tomiyama Y. Glanzmann thrombasthenia: integrin $\alpha_{IIb}\beta_3$ deficiency. *Int J Hematol* 2000; **72**: 448–54.
6 Coller BS. Platelet GPIIb/IIIa antagonists: the first anti-integrin receptor therapeutics. *J Clin Invest* 1997; **99**: 1467–70.
7 Topol EJ, Byzova TV, Plow EF. Platelet GPIIb-IIIa blockers. *Lancet* 1999; **353**: 227–31.
8 Takagi J, Petre B, Walz T, Springer T. Global conformational rearrangements in integrin extracellular domains in outside-in and inside-out signaling. *Cell* 2002; **110**: 599–611.
9 Xiong JP, Stehle T, Goodman SL, Arnaout MA. New insights into the structural basis of integrin activation. *Blood* 2003; **102**: 1155–9.
10 Peerschke EIB. Ca^{+2} mobilization and fibrinogen binding of platelets refractory to adenosine diphosphate stimulation. *J Lab Clin Med* 1985; **106**: 111–22.
11 van Willigen G, Akkerman JW. Regulation of glycoprotein IIB/IIIA exposure on platelets stimulated with α-thrombin. *Blood* 1992; **79**: 82–90.
12 Gachet C. ADP receptors of platelets and their inhibition. *Thromb Haemost* 2001; **86**: 222–32.
13 Dorsam RT, Kunapuli SP. Central role of the $P2Y_{12}$ receptor in platelet activation. *J Clin Invest* 2004; **113**: 340–5.
14 Fabre JE, Nguyen M, Latour A, Keifer JA, Audoly LP, Coffman TM, Koller BH. Decreased platelet aggregation, increased bleeding time and resistance to thromboembolism in $P2Y_1$-deficient mice. *Nat Med* 1999; **5**: 1199–202.
15 Hollopeter G, Jantzen HM, Vincent D, Li G, England L, Ramakrishnan V, Yang RB, Nurden A, Julius D, Conley PB. Identification of the platelet ADP receptor targeted by antithrombotic drugs. *Nature* 2001; **409**: 202–7.
16 Foster CJ, Prosser DM, Agans JM, Zhai Y, Smith MD, Lachowicz JE, Zhang FL, Gustafson E, Monsma Jr FJ, Wiekowski MT, Abbondanzo SJ, Cook DN, Bayne ML, Lira SA, Chintala MS. Molecular identification and characterization of the platelet ADP receptor targeted by thienopyridine antithrombotic drugs. *J Clin Invest* 2001; **107**: 1591–8.
17 Shiraga M, Miyata S, Kato H, Kashiwagi H, Honda S, Kurata Y, Tomiyama Y, Kanakura Y. Impaired platelet function in a patient with $P2Y_{12}$ deficiency caused by a mutation in the translation initiation codon. *J Thromb Haemost* 2005; **3**: 2315–23.
18 Shattil SJ, Hoxie JA, Cunningham M, Brass LF. Changes in the platelet membrane glycoprotein IIb-IIIa complex during platelet activation. *J Biol Chem* 1985; **260**: 11107–14.
19 Maruyama K, Kinami J, Sugita Y, Takada Y, Sugiyama E, Tsuchihashi H, Nagatomo T. MCI-9042: high affinity for serotonergic receptors as assessed by radioligand binding assay. *J Pharmacobiodyn* 1991; **14**: 177–81.
20 Tokuhira M, Handa M, Kamata T, Oda A, Katayama M, Tomiyama Y, Murata M, Kawai Y, Watanabe K, Ikeda Y. A novel regulatory epitope defined by a murine monoclonal antibody to the platelet GPIIb-IIIa complex ($\alpha_{IIb}\beta_3$ integrin). *Thromb Haemost* 1996; **76**: 1038–46.
21 Honda S, Tomiyama Y, Aoki T, Shiraga M, Kurata Y, Seki J, Matsuzawa Y. Association between ligand-induced conformational changes of integrin $\alpha_{IIb}\beta_3$ and $\alpha_{IIb}\beta_3$-mediated intracellular Ca^{2-} signaling. *Blood* 1998; **92**: 3675–83.
22 Shiraga M, Tomiyama Y, Honda S, Suzuki H, Kosugi S, Tadokoro S, Kanakura Y, Tanoue K, Kurata Y, Matsuzawa Y. Involvement of Na^+/Ca^{2+} exchanger in inside-out signaling through the platelet integrin $\alpha_{IIb}\beta_3$. *Blood* 1998; **92**: 3710–20.
23 Nylander S, Mattsson C, Ramstrom S, Lindahl TL. The relative importance of the ADP receptors, P2Y12 and P2Y1, in thrombin-induced platelet activation. *Thromb Res* 2003; **111**: 65–73.
24 D'Souza L, Glueck HI. Measurement of nucleotide pools in platelets using high pressure liquid chromatography. *Thromb Haemost* 1977; **38**: 990–1001.
25 Hardy AR, Conley PB, Luo J, Benovic JL, Poole AW, Mundell SJ. $P2Y_1$ and $P2Y_{12}$ receptors for ADP desensitize by distinct kinase-dependent mechanisms. *Blood* 2005; **105**: 3552–60.
26 Baurand A, Eckly A, Hechler B, Kauffenstein G, Galzi JL, Cazenave JP, Leon C, Gachet C. Differential regulation and relocalization of the platelet P2Y receptors after activation: a way to avoid loss of hemostatic properties? *Mol Pharmacol* 2005; **67**: 721–33.
27 Bertoni A, Tadokoro S, Eto K, Pampori N, Parise LV, White GC, Shattil SJ. Relationships between Rap1b, affinity modulation of integrin $\alpha_{IIb}\beta_3$, and the actin cytoskeleton. *J Biol Chem* 2002; **277**: 25715–21.
28 Crittenden JR, Bergmeier W, Zhang Y, Piffath CL, Liang Y, Wagner DD, Housman DE, Graybiel AM. CalDAG-GEFI integrates signaling for platelet aggregation and thrombus formation. *Nat Med* 2004; **10**: 982–6.
29 Chrzanowska-Wodnicka M, Smyth SS, Schoenwaelder SM, Fischer TH, White GC. Rap1b is required for normal platelet function and hemostasis in mice. *J Clin Invest* 2005; **115**: 680–7.
30 Andre P, Delaney SM, LaRocca T, Vincent D, DeGuzman F, Jurek M, Koller B, Phillips DR, Conley PB. $P2Y_{12}$ regulates platelet adhesion/activation, thrombus growth, and thrombus stability in injured arteries. *J Clin Invest* 2003; **112**: 398–406.
31 Lova P, Paganini S, Sinigaglia F, Balduini C, Torti M. A G_i-dependent pathway is required for activation of the small GTPase Rap1B in human platelets. *J Biol Chem* 2002; **277**: 12009–15.
32 Woulfe D, Jiang H, Mortensen R, Yang J, Brass LF. Activation of Rap1B by G_i family members in platelets. *J Biol Chem* 2002; **277**: 23382–90.
33 Heptinstall S, Johnson A, Glenn JR, White AE. Adenine nucleotide metabolism in human blood – important roles for leukocytes and erythrocytes. *J Thromb Haemost* 2005; **3**: 2331–9.
34 Remijn JA, Wu YP, Jeninga EH, IJsseldiik MJ, van Willigen G, de Groot PG, Sixma JJ, Nurden AT, Nurden P. Role of ADP receptor $P2Y_{12}$ in platelet adhesion and thrombus formation in flowing blood. *Arterioscler Thromb Vasc Biol* 2002; **22**: 686–91.
35 Kulkarni S, Dopheide SM, Yap CL, Ravanat C, Freund M, Mangin P, Heel KA, Street A, Harper IS, Lanza F, Jackson SP. A revised model of platelet aggregation. *J Clin Invest* 2000; **105**: 783–91.
36 Massberg S, Gawaz M, Gruner S, Schulte V, Konrad I, Zohlnhofer D, Heinzmann U, Nieswandt B. A crucial role of glycoprotein VI for platelet recruitment to the injured arterial wall in vivo. *J Exp Med* 2003; **197**: 41–9.

Thrombosis Research (2007) 119, 35–43

ELSEVIER

THROMBOSIS RESEARCH

intl.elsevierhealth.com/journals/thre

REGULAR ARTICLE

Haplotype of thrombomodulin gene associated with plasma thrombomodulin level and deep vein thrombosis in the Japanese population

Shoko Sugiyama [a,b], Hisao Hirota [a,✝], Rina Kimura [b], Yoshihiro Kokubo [c], Tomio Kawasaki [d,*], Etsuji Suehisa [e], Akira Okayama [c], Hitonobu Tomoike [c], Tokio Hayashi [f], Kazuhiro Nishigami [f], Ichiro Kawase [g], Toshiyuki Miyata [b]

[a] *Department of Cardiovascular Medicine, Osaka University Graduate School of Medicine, 2-2, Yamadaoka, Suita City, Osaka 565-0871, Japan*
[b] *Research Institute, National Cardiovascular Center, Japan*
[c] *Department of Preventive Cardiology, National Cardiovascular Center, Japan*
[d] *Cardiovascular Surgery, Osaka University Graduate School of Medicine, Japan*
[e] *Department of Laboratory Medicine, Osaka University Hospital, Japan*
[f] *Department of Cardiology, National Cardiovascular Center, Japan*
[g] *Respiratory Medicine and Rheumatic Diseases, Osaka University Graduate School of Medicine, Japan*

Received 9 December 2005; received in revised form 19 December 2005; accepted 20 December 2005
Available online 28 February 2006

KEYWORDS
Thrombomodulin;
Deep vein thrombosis;
Gene mutations;
Soluble thrombomodulin;
Japanese;
Case-control study

Abstract

Introduction: Thrombomodulin (TM) is an essential cofactor in protein C activation by thrombin. Here, we evaluated the contribution of genetic variations in the TM gene to soluble TM (sTM) level and deep vein thrombosis (DVT) in Japanese.
Patients and methods: We sequenced the TM putative promoter, exon, and 3′-untranslated region in DVT patients ($n=118$). Among 17 genetic variations we identified, two missense mutations (R385K, D468Y) and three common single nucleotide polymorphisms (−202G>A, 2487A>T, 2729A>C) were genotyped in a general population of 2247 subjects (1032 men and 1215 women) whose sTM levels were measured. We then compared the frequency of these mutations in DVT patients

Abbreviations: DVT, deep vein thrombosis; TM, thrombomodulin; PC, protein C; APC, activated protein C; PS, protein S; EGF, epidermal growth factor; SNP, single-nucleotide polymorphism; sTM, soluble TM; 5′-UTR, 5′-untranslated region; 3′-UTR, 3′-untranslated region.

* Corresponding author. Tel.: +81 6 6879 3251; fax: +81 6 6879 3259.
E-mail address: kawasaki@sug2.med.osaka-u.ac.jp (T. Kawasaki).
✝ Deceased.

doi:10.1016/j.thromres.2005.12.012

with that in the age, body mass index-adjusted population-based controls.
Results: We identified one neutral mutation (H381) and three missense mutations (R385K; $n=2$, A455V; $n=53$ heterozygous, $n=14$ homozygous, D468Y; $n=2$) of TM in the DVT patients. Age-adjusted mean values of sTM were lower in C-allele carriers of 2729A>C than in noncarriers in the Japanese general population (women: 16.7 ± 0.3 U/ml vs. 17.9 ± 0.2 U/ml, $p<0.01$, men: 19.4 ± 0.3 U/ml vs. 20.4 ± 0.3 U/ml, $p=0.03$). Additionally, the CC genotype of this mutation was more common in the male DVT patients than in the male individuals of the general population (odds ratio=2.76, 95% confidence interval=1.14–6.67; $p=0.02$). This mutation was in linkage disequilibrium (r-square>0.9) with A455V mutation.
Conclusions: TM mutations, especially those with a haplotype consisting of 2729A>C and A455V missense mutation, affect sTM levels, and may be associated with DVT in Japanese.

Introduction

Family-based studies have established that venous thromboembolism is, at least in part, an inherited disease with estimated heritabilities of approximately 60% [1,2]. The mode of inheritance of venous thromboembolism is probably complex [2]. Moreover, family-based and twin studies have established that over 25 plasma hemostasis-related analytes (traits) both correlate with thrombosis and are heritable [3–5]. In Caucasians, the factor V-Leiden mutation and prothrombin G20210A mutation are widely recognized as genetic risk factors for deep vein thrombosis (DVT) [6]. However these mutations are not present in the Japanese [7,8]. Recently, we and others found that the protein S (PS) K196E mutation, known as the PS Tokushima mutation, is a genetic risk for DVT in the Japanese population, indicating large differences in the genetics of DVT among ethnicities [9,10].

Thrombomodulin (TM) is a transmembrane protein that is constitutively expressed on the luminal surface of vascular endothelial cells [11]. The anticoagulant function of TM is mediated by interaction with thrombin and protein C (PC). Endothelial membrane-bound TM forms a high-affinity complex with thrombin via thrombin exosite 1, and inhibits thrombin interaction with fibrinogen and protease-activated receptor-1. In contrast, the thrombin–TM complex is a potent activator of PC, and TM enhances thrombin-dependent PC activation by more than two orders of magnitude. Due to the abundance of TM in the microvasculature, the vast majority of thrombin generated under ambient conditions is sequestered by TM. Constitutive inhibition of the procoagulant function of thrombin and tonic formation of activated PC (APC) comprise an essential anticoagulant mechanism that prevents the amplification of thrombin generation, via proteolysis of activated coagulation factors Va and VIIIa by APC.

TM encoded by an intron-less gene consists of a large N-terminal extracellular region, a single transmembrane segment, and a short cytoplasmic tail [12]. The extracellular region is comprised of an N-terminal lectin-like domain followed by six tandem repeats of epidermal growth factor (EGF)-like domains, and a glycosylated (chondroitin sulfate) serine/threonine-rich domain. The thrombin-binding region has been localized to the fifth and sixth EGF-like domains, while the fourth EGF-like domain is required for PC binding to the thrombin–TM complex. The serine/threonine-rich spacer region is required for both thrombin binding and TM cofactor activity for membrane-associated TM. The chondroitin sulfate domain may stabilize thrombin binding to TM, possibly by interacting with the thrombin apolar region [13,14].

Animal model data suggest that TM dysfunction or deficiency is associated with a prothrombotic disorder. Knock-in mice with a TM mutant that has a mutation corresponding to human E387P exhibit a prothrombotic disorder [15]. This amino acid change is located between the interdomain loop of the fourth and fifth EGF-like domains and abolishes the ability of soluble TM (sTM) to catalyze in vitro thrombin activation of PC to APC. Mice with TM deficiency limited to the vascular endothelium die shortly after birth as a result of a consumptive coagulopathy that can be prevented by warfarin anticoagulation [16].

Based on the important antithrombotic role of TM, we hypothesized that genetic variations within the TM gene that alter TM expression and/or impair anticoagulant function could predispose to venous thromboembolism. To test this hypothesis, we screened the promoter, exon, and 3′ -untranslated regions (3′ -UTR) of the TM gene in unrelated patients with idiopathic, objectively confirmed